FEATURES OF SLIP PHENOMENON IN DOUBLE STRATIFIED FLUID FLOW WITH VISCOUS DISSIPATION

By

ADEEL AHMAD

NATIONAL UNIVERSITY OF MODERN LANGUAGES

ISLAMABAD

July, 2023

FEATURS OF SLIP PHENOMENON IN DOUBLE STRATIFIED FLUID FLOW WITH VISCOUS DISSIPATION

By

ADEEL AHMAD

MS MATH, National University of Modern Languages, Islamabad, 2023

A THESIS SUBMITTED IN PARTIAL FULFILMENT OF

THE REQUIREMENTS FOR THE DEGREE OF

MASTER OF SCIENCE

In **Mathematics**

To

FACULTY OF ENGINEERING & COMPUTER SCIENCE

NATIONAL UNIVERSITY OF MODERN LANGUAGES ISLAMABAD

THESIS AND DEFENSE APPROVAL FORM

The undersigned certify that they have read the following thesis, examined the defense, are satisfied with overall exam performance, and recommend the thesis to the Faculty of Engineering and Computer Sciences for acceptance.

Thesis Title: Features of Slip phenomenon in Double Stratified Fluid Flow with Viscous Dissipation

Submitted By: Adeel Ahmad **Registration #:** 07 MS/MATH/S20

Master of Science in Mathematics (MS MATH)
Title of the Degree

MATHEMATICS
Name of Discipline

Dr. Aisha Anjum _____
Name of Research Supervisor Signature of Research Supervisor

Dr. Sadia Riaz _____
Name of HOD (MATH) Signature of HOD (MATH)

Dr. Noman Malik _____
Name of Dean (FE&CS) Signature of Dean (FE&CS)

July 21th, 2023

AUTHOR'S DECLARATION

I Adeel Ahmad

Son of Muhammad Ramzan

Registration # 07 MS/MATH/S20

Discipline Mathematics

Candidate of **Master of Science in Mathematics (MS MATH)** at the National University of Modern Languages do hereby declare that the thesis **Features of Slip phenomenon in Double Stratified Fluid Flow with Viscous Dissipation** submitted by me in partial fulfillment of MS Math degree, is my original work, and has not been submitted or published earlier. I also solemnly declare that it shall not, in future, be submitted by me for obtaining any other degree from this or any other university or institution. I also understand that if evidence of plagiarism is found in my thesis/dissertation at any stage, even after the award of a degree, the work may be cancelled and the degree revoked.

Signature of Candidate

Adeel Ahmad

Name of Candidate

21th July, 2023

Date

ABSTRACT

Title: Features of Slip phenomenon in Double Stratified Fluid Flow with Viscous Dissipation

The dissertation investigates the steady motion of an incompressible viscous fluid on a sheet caused by a stretching phenomenon under the influence of magnetic field. The porous medium effects are also retained in the analysis. Here, features of mass and heat transport are described in terms of viscous dissipation, joule heating and double stratification phenomena. The slip conditions (i.e. velocity, thermal and solutal) are accounted in the current analysis. The governing equations are made dimensionless by implementing suitable variables. The convergent solutions are acquired by utilizing a homotopic technique. Surface heat transfer rate and drag force are elaborated to corresponding few important parameters. As conclusion, it is depicted that dominant stratification phenomenon decays both temperature and concentration fields.

TABLE OF CONTENTS

LIST OF FIGURES

LIST OF ABBREVIATIONS

2D	-	Two dimensions
3D	-	Three dimensions
ODE	-	Ordinary Differential Equation
PDE	-	Partial Differential Equation
IVP	-	Initial value Problem
BVP	-	Boundary value Problem
MHD	-	Magnetohydrodynamic
HAM	-	Homotopy Analysis Method

LIST OF SYMBOLS

x, y	Cartesian Coordinate
$\tilde{u}, \tilde{v}$	Velocity Component
B_0	Magnetic Parameter
ϵ	Velocity Ratio Parameter
α	Thermal diffusivity
k	Thermal conductivity
B	Magnetic Field
Ω	Permeability Parameter
ν	Kinematic viscosity
ρ	Density
K	Permeability of porous medium
C_p	Specific heat
Q_0	Heat generation and absorption coefficient
M	Magnetic field strength
$\tilde{T}$	Temperature
$\tilde{C}$	Concentration
$\widetilde{U}_w$	Stretching velocity
$\tilde{C}_w$	Concentration at wall
$\tilde{T}_w$	Temperature at wall
$\widetilde{U}_\infty$	Free stream velocity
$\tilde{T}_\infty$	Ambient fluid temperature
$\tilde{C}_\infty$	Ambient fluid concentration
$\tilde{V}_w$	Constant suction and injection
s_1	Velocity slip
s_2	Thermal slip
s_3	Solutal slip
ϵ_1	Thermal stratification
ϵ_2	Solutal stratification

Re	Reynold number
Sc	Schmidt number
Nu	Nusselt number
P_r	Prandtl number
Ec	Eckert number

ACKNOWLEDGMENT

First of all, I wish to express my gratitude and deep appreciation to Almighty **Allah**, who made this study possible and successful. This study would not be accomplished unless the honest espousal that was extended from several sources for which I would like to express my sincere thankfulness and gratitude. Yet, there were significant contributors for my attained success, and I cannot forget their input, especially my research supervisors, **Dr. Aisha Anjum**, who did not leave any stone unturned to guide me during my research journey.

I shall also acknowledge the extended assistance from the administrations of Department of Mathematics who supported me all through my research experience and simplified the challenges I faced. For all whom I did not mention but I shall not neglect their significant contribution, thanks for everything.

DEDICATION

This thesis work is dedicated to my parents and my teachers throughout my education career who have not only loved me unconditionally but whose good examples have taught me to work hard for the things that I aspire to achieve

CHAPTER 1

INTRODUCTION

In practical life applications, boundary layer flows perform an important role particularly when body and fluid are in contact. Due to drag/friction forces, a skinny layer generates on the objects surface referred as boundary layer. These forces are dominant in turbulent boundary layer in evaluation comparison to laminar boundary layer. Now-a-days, scientists and researchers are interested to enhance the efficiency of various machines and technologies via decaying drag/friction forces. Discount of such forces may be achieved with the aid of fending off boundary layer from separation, through motion of the item, permeable sheet, heating or cooling of sheet and body forces. Thus, characteristics of heat in flow of boundary layer similar to moving surfaces have massive applications in biological and engineering manufacturing techniques. These programs involve hot rolling, productions of glass fiber and paper; twine drawing, spinning of metals, polymer extrusion, and many others.

Stratification occurs as a result of temperature fluctuations, concentration differences, or different liquids with different densities. Researchers and scientists are interested in studying the properties of stratification because of its wide range of applications in engineering, industry, agriculture, biomedical, and natural processes. There are several examples of stratification, including stratification in storage tanks, oceans, rivers, streams, waterfalls, and heterogeneous mixtures of the atmosphere. Homogeneous mixtures and product performance control require stratification. It plays an important role in controlling hydrogen and oxygen levels in the atmosphere and oceans. It has a significant impact on algal abundance, water quality, and dissolved oxygen deficiency in the lower reaches of rivers, lakes, and ponds. Stratification is related to fluid flow due to temperature and concentration changes present on the surface of an object or in the environment. Further, it is mainly classified into linear and nonlinear stratification. To disclose the features of fluid flows, we can't collect the accurate data and never approach the exact solutions and behaviors of fluids without stratification. By stratification process, we can make stable and homogeneous mixtures of various fluids which are most important in the industrial processes and quantity of heat can be calculated accurately for heating purpose of such fluids and quality of final products mainly depends on

this phenomenon. Stratification in biomedical area can be used to prevent the clotting of blood which is the more important factor of the stratification to save the lives of patients.

Investigating the traits of fluid flow over an impermeable or rigid body, the point at which the velocity of the fluid particles is zero, i.e., the flow that stops at the surface of the body is called the stagnation point, and the flow near the stagnation point is called the stagnation point flow. Furthermore, he of (a) orthogonal stagnation points and (b) oblique stagnation points can be divided into two types. At orthogonal stagnation points, the fluid particles act perpendicular/perpendicular to the surface of the rigid frame, resulting in tempo vanishing at one point. However, at oblique stagnation points, the fluid particles originate obliquely on the rigid frame from any point of view. Indirect stagnation points are mentioned for miles including orthogonal stagnation and shear flows parallel to the body. Stagnation point flows exist as two- or three-dimensional, non-steady or steady, viscous or in viscous, asymmetric or symmetric, regular or oblique, uneven or uniform, and forward or backward fluid. Stagnation point flow properties play an important role in engineering, biomedicine, and natural phenomena, such as flows descending over submarines, missiles, oil ships, and aircraft. Stagnation points also serve an important function in biomedical technology via blood circulation at junctions within arteries.

The study of fluid dynamics has always been a subject of great interest to scientists and researchers with respect to widespread applications in various fields of engineering, industrial, geophysical, biomedical and pharmaceutical processes. The reason behind this is “the rapid utilization of liquids and gases in these processes”. These fluids are mainly categorized into main two types i.e., Newtonian and non-Newtonian fluids. In Newtonian fluids, shear stress has related linearly and directly with deformation rate, however, in non-Newtonian fluids this relation becomes nonlinear. The features of non-Newtonian fluids cannot be described by the single empirical expression due to their diverse microstructure in nature. So, every non-Newtonian model has their own mathematical model corresponding to relevant characteristics. Blood, ketchup, toothpaste, polymers, ink, nail polish, honey etc. exemplify the non-Newtonian fluids. Such fluids play significant impact in the presence of slip conditions. Slip conditions refer to the difference in velocity between fluid particles and the plate surface. One of the most important applications of studying slip conditions is in the development of artificial hearts. Understanding the behavior of blood flow in tubes and channels is crucial for designing effective artificial hearts that can mimic the natural flow of

blood in the human body. Another important application is in reducing surface friction, which can lead to significant energy savings in industrial processes. This can also be used for conserving renewable energy. An important aspect of studying slip conditions is the inclusion of temperature and concentration slips. These slips reflect real-world conditions and are commonly observed in natural, manufacturing, technological, and biological processes. The presence of temperature and concentration slips significantly enhance the role of studying velocity slip as they are often present in the natural and technological environment. Thus, understanding the behavior of fluid moving across a surface with boundary slip is essential for making advancements in various fields, including artificial hearts, accurate blood flow analysis, reducing surface friction, and conserving renewable energy. The modest wall slip condition that particular polymeric melts exhibit is often governed by a monotonic relationship between slip velocity and adhesion. In such a context, the slip boundary condition, which is described as a phenomenon in which the velocity of fluid particles differs from the velocity of a plate. Scientists have shown their keen interest in decaying the skin friction constant and consequently the speed of heating or cooling in present technological processes. Various attempts to reduce skin friction or drag forces for flows over the surface of a wing, tail plane, and wind turbine rotor have been made. However, by delaying the transition from laminar fluid flow to transition fluid flow and preventing the boundary layer from splitting, a decrease in force is generated. There are several methods that may be used to vanish this task. Examples include altering the surface, using injection, and creating suction by using body forces. The design of bearings, radial use clogging, and thermal oil recovery are all examples of suction and blowing processes in engineering. Injection is employed to reduce plate temperatures, lessen surface friction, and avoid rusting.

Viscous dissipation refers to the energy wastage due to resistance between fluid particles which greatly depends on the microstructure behavior of various fluids. Further, viscous dissipation is dominant in those fluids which have strong cohesive forces i.e., strong intermolecular forces or consequently strong viscous forces. In real life there exist no such fluid which has zero viscous dissipation. It is noted that convective flow strongly depends on the viscosity of the fluid and alternatively have a significant role in the rate of heat transfer. Higher viscous dissipation grows the thermal boundary layer in fluid flows. This growing behavior of thermal boundary layer enhances the temperature of the systems in industrial processes which in turn decays the life cycle of the machinery. This is economically

unsuitable for any running industry and cannot support the renewable energy resources. To save the renewable energy resources viscous dissipation may be minimized.

The properties of magnetohydrodynamic (MHD) fluid flow play an important role in many industrial and commercial processes. Such processes include the design of nuclear reactors, liquid metal cooling systems, blood flow measurements, pumps, MHD turbines, and more. It is also used in thermal reactors to control the diffusion rate of neutrons. However, electromagnetic forces can be applied to modulate the electrical conduction of fluid flow. This compensates for the lack of momentum in the boundary layer. Highly conductive liquids are more likely to be disturbed by implementing an external magnetic field of approximately 1 Tesla. This concept is used to manipulate flows in classical magnetohydrodynamics. More precisely, MHD is the study of magnetic fluid dynamics and fluids that contain electrically conducting particles. Magneto fluids include plasma, liquid metal, and conducting fluids. The words magnetohydrodynamic and hydrodynamic stand movement are invented from the word's magneto and hydro. The essential principle underpinning MHD is that magnetic fields have the capacity to generate currents in flowing conductive fluids, which polarize the fluid and hence change the magnetic properties. Examples of hydromagnetic applications include blood flow within tissues, boundary layers along material conveyers, and aerodynamic extrusion of plastic sheets.

Boundary conditions have a decisive influence on the material processing of technology and have a great influence on the properties of the final product. In the literature, his one type of boundary condition is commonly studied: slip resistance at boundaries. There is another type of boundary condition called a slip situation where the velocity of the fluid at a stable boundary is non-zero with respect to the boundary. However, in a real lifestyle program, non-slip situations do not always apply. His miles are lacking in various herbal, business, and bioengineering techniques. Such processes include anomalous velocities of bodies and liquid particles tested as boundary slip. Liquid leakage occurs in exceptional circumstances such as low-cost lubrication, polishing of internal cavities and synthetic heart valves, optical coatings, and cooling systems. As a result, slack constraints have gained considerable appeal for researchers. The process of directing liquid flow through stretchable films has attracted the attention of many scientists and researchers. Tuning of heat transfer properties in the presence of stretch films. There is an extensive design and technology package for fluids passing through ductile plates. Hot rolling, wire tinning, extrusion batches, papermaking, food

processing, fiberglass, and various metallurgical batches are examples of these types of fluid streams.

The heat transfer mechanism is the transport of thermoelectricity from a warm body to a cold body. Heat transfer between a body and its surroundings or other bodies while maintaining the temperature difference between them is also called heat transfer. In this way, it happens that the environment and the body reach thermal equilibrium. According to the 2D rules of thermodynamics, heat is continuously transferred from a warm body to a cold body. Traditionally, heat intensity transfer occurs only through radiation, conduction, convection, or a mixture of these. Heat transfer involving matter consisting of partial heat exchange (consisting of the transfer of boiling heat by means of steam). The term mass transfer is commonly used in the engineering of physical strategies involving molecular and convective transport of atoms (and molecules) within physical systems. Adapts to the liquid flow and operation of the separation unit. There are many similarities that can be observed in mass, heat, and molecular power. Fick's Law of Change of Mass, Fourier's Law of Heat Transfer, and Newton's Law of Change of Momentum are very similar. Therefore, these molecular switching tactics have many similarities. Differences in attentiveness predict usage pressure for mass mailing. Random molecular motion contributes to the net delivery of mass from areas of high consciousness to areas of low consciousness. Bulk transfer size can be determined by calculating and applying bulk mail co-green. The results of mass exchange are of great importance in the evaporation of water from the field to the environment, the distillation of blood in the kidneys and liver, and the purification of alcohol. Thermal cycling and mass cycling sequences play an important role in large-scale applications in engineering, bodybuilding, and industry. These applications include mist formation and distribution, construction of many chemical processing plants, agricultural fields, temperature and humidity distribution in orchards, crop damage from freezing, environmental pollutants, drying of porous solids, geothermal Reservoirs, packaged mattresses, catalytic reactors, insulation, improved oil recovery and underground power supply.

Boundary layer swimming is very important under conditions of direct contact between the liquid and the frame. E. When liquid flows across the floor. A thin boundary layer is formed in which the fluid modulates the speed of the frame through friction/drag. The effect of such forces is smaller in a laminar boundary layer than in a turbulent boundary layer. Researchers today are trying to improve the efficiency of various machines by reducing drag/friction

forces. Accordingly, various attempts have been made to reduce the drag on lift forces from the ground, such as tailplanes, wings, and rotors of wind turbines. However, such forces can be reduced by moving the boundary layer away from separation and shifting the transition from laminar to turbulent. This task can be accomplished through specific body elements and surface transport, fluid suction and injection, the presence of body forces, and soil cooling/heating. Therefore, the analysis of boundary layer flow heat transfer by transfer surfaces has a wide scope in commercial production processes. Some examples of such processes include fiberglass manufacturing, hot rolling, papermaking, wire drawing, continuous casting, metal spinning, metal and polymer extrusion, and plastic film drawing. The final product of copper wire annealing and thinning is greatly dependent on the price of heat switches on the stretched surface. Such flow behavior in the presence of magnets plays a central role within metallurgical processes. Cooling performance can be created by drawing strips with a magnetohydrodynamic (MHD) fluid and the desired material. At best, the kinematics of stretching and simultaneous heating or cooling have a large impact on the final product. The four exclusive heat transfer phenomena from the wall to the surrounding fluid were originally considered by Merkin. These are (a) normal or specified bed temperature, (b) constant or specified bed heat flux, (c) conjugate limit situations, and (d) Newtonian heating where the heat exchange from the interface is finite heat. Consists of Proportional to local floor temperature. The researchers applied the Newtonian heating method to a practical package, along with heat exchangers, conjugate heat transfer round fins, and convection where the interface absorbs heat via solar radiation.

In recent years, the improvement of human society is highly dependent on energy sources. Researchers and scientists are interested in exploring new power sources and energy technologies for harnessing solar energy (approximately 4×10^{15} MW to reach Earth). This solar power is 2000 times more than the world's electricity consumption. Nanostructures (nanoclusters) were first used by Choi to improve the thermal conductivity and strength retention of liquids. Solar heat is very suitable for various heating methods in industry and technology and can be a portable and easy-to-use heat source. Such an approach cannot rely on the power of limited resources. A solar collector is a tool designed to convert solar radiation into heat energy. This heat flow is absorbed by existing materials in the solar collector. Solar energy can be used to heat water, but the difficulty with this technology is that water is used as the energy carrier for solar cells, which makes it less efficient. Water has a

low heat transfer coefficient because it has a thermophilically negative house. Therefore, to improve the performance of such devotees, an entirely new kind of liquid of magnificence, known as nano liquid, was investigated. A nanofluid is a combination of a base fluid and nanoparticles. Used to beautify thermal switches in microelectronics, microchips in computer systems, gasoline batteries, transportation, biomedical, food processing, strong rural lighting, and manufacturing costs. Largest liquids including water, ethylene, glycol oil, etc. Low thermal conductivity. Suspended nano-sized metal flakes (titanium, copper, gold, iron or their oxides) are used to increase the thermal conductivity of such materials. Nanoparticles come in a variety of shapes, such as round, rod-like, and tubular.

Transfer of heat and mass is treated from time to time as one-of-a-kind shape of convection warmth and mass delivery. Convection occurs in unique form consist of herbal and pressured convection. In a few warmness and mass transport structures, both forced and natural convections make a contribution substantially to the charge of warmth and mass transfer. Differences in temperature and attention are now very large in double diffusive mixed convection, depending on the orientation and heating conditions provided. This property seems to arise from recognizing temperature fluctuations and high or very low swimming speeds. Indeed, the velocity, temperature and concentration profiles within the buoyancy layer are exchanged between the liquid and the soil with the buoyant force acting as a pressure gradient and the Nusselt and Sherwood numbers. However, various commercial strategies combined, in addition to wind-exposed solar receivers, emergency-shutdown-cooled nuclear reactors, fan-cooled digital equipment, and heat exchangers in low-velocity environments. Motivated by convection.

Recent advances in Darcy regulation resulting from fluid flow through porous media have attracted the attention of the research community from a practical point of view. This leads to porous layer overflow and seepage in commercial and botanical problems. These include natural groundwater flows, vitamins in flowers, oils through porous bedrock, and blood flow in animal tissues. Similarly, flotation through porous layers or plates (surfaces) can be applied to various applications such as engine coolers, lubrication mechanisms, cooling and heating system layouts, and designing porous surfaces in this way to reduce drag. It is also encountered in business methods (i.e., Airplane wings with porous cavities) and gas and oil production. Focuses on production estimation and optimization. Fluid flow in porous media can often be calculated by applying Darcy's law. At high speeds, however, Darcy's scheme is

very difficult to describe fluid flow. If one wanted to circumvent the deficiencies of the Darcian rule, Forchheimer introduced his second term called the non-Darcy term. This includes apparent velocity, liquid density, and non-Darcy coefficients.

Brief summary and structure of this thesis is provided below to assist readers:

Chapter 2 provides detailed literature review related to the work discussed comprehensively in Chapter 1.

Chapter 3 provides an overview of basic definitions, terminologies, and fundamental laws related to the study of fluid dynamics, including dimensionless numbers.

Chapter 4 presents an extensive evaluation of the published work. It explores the deformed and incompressible viscous fluid flow caused by a stagnation point on a linearly stretched sheet. A normal magnetic field is applied to a porous surface. This chapter further develop the heat transportation via energy absorption and production. Through suitable transformations, the resultant Navier-Stokes equations are provided in non-dimensional form, and converging solutions are calculated with the use of a homotopic approach. Graphical behavior of temperature and velocity are discussed comprehensively through various physical parameters. Drag or skin friction at the surface is evaluated through emerging parameters. The thermal and velocity of fluid particles have declining behavioral for the dominant Prandtl number and magnetic field parameter.

Chapter 5 addresses the properties of a continuous, incompressible flow of viscous fluid distorted over a horizontally oriented, linearly stretchable sheet. A magnetic field is applied to a permeable sheet in two-dimensional vertical flow. Additionally, characteristics of continuous temperature and concentration transmission along with resistive heating, viscous dissipation, and linear dual stratified fluid flow are investigated comprehensively. The velocity, temperature, and concentration slip conditions applied to the solid surface within the boundary layer problem. The governing equations transformed through suitable transformations and analytical convergent solutions are deals with using the homotopic technique. The graphical and physically examination of heat, velocity, and concentration fields are discussed extensively by using various emerging parameters. Heat exchange rate of a solid surface and skin friction drag in the context of the relevant parameters. Finally, the fundamental stratified phenomenon diminishes overall the concentrations and thermal fields.

Chapter 6 describes the general conclusions and future work.

CHAPTER 2

LITERATURE REVIEW

This chapter describes the detailed overview of the articles related to boundary layer, stratification, stagnation point, Newtonian and non-Newtonian fluids, slip phenomenon and magnetohydrodynamic flows.

Merkin and Kumaran [1] presented the unsteady flow of viscous fluid located over an infinite long sheet. The flow features in the boundary-layer via shrinking surface in an electrically accomplishing fluid are investigated. The nature of the solution is proven to depend upon a dimensionless magnetic parameter. Boundary layer continuously occurred for all the time. However, its thickness grows for large time and decays for dominant magnetic field. Although skin friction remains finite for large time scale solutions. Escott and Griffiths [2] discussed the properties of boundary layer formed in the viscoelastic fluids. They have shown that each the fluid speed inside the boundary layer and the pressure at the strong boundary boomed due to the impact of viscoelasticity. Attributable to this, they expected a thinning of the boundary layer because the cost of the dimensionless viscoelastic go with the flow parameter is accelerated. Those outcomes contradicted a number of distinguished research within the literature i.e., boundary layer decays gradually due to dominant viscoelastic parameter. Kousar and Liao [3] explored the characteristics of non-similar behavior of boundary layer generated through impulsively stretching surface. The resulting governing equations are made dimensionless through suitable transformations. The solutions are tackled through homotopic technique. Merkin and Kumaran [4] scrutinized the characteristics of free convection in boundary layer region in the vicinity of stagnation point through porous material. Three forms for the wall boundary situation are dealt with i.e., a prescribed wall temperature, prescribed wall heat flux and Newtonian heating. In each case the flow and temperature equations are reduced by a dimensionless parameter δ at which the fluid attained its density maximum. Bhattacharyya *et al.* [5] studied the slip features in boundary layer over a heated and stretchable flat sheet through porous material. Due to existence of porous plate, fluid speed enhanced while non-dimensional

temperature decreased for dominant values of suction parameter but it enhanced with increasing blowing parameter. Their evaluation revealed that the growth of speed slip parameter reduced the momentum boundary layer thickness and also complements the heat switched from the plate. However, temperature decreased with thermal slip parameter. Khan and Azam [6] explored the behavior of boundary layer formed Carreau fluid located over the permeable and stretchable surface. The dimensionless governing equations are solved through Bvp4c. They concluded that decrement occurred in the boundary layer for higher unsteadiness and mass transfer parameter. Rauf *et al.* [7] analyzed the MHD mixed convective boundary layer flow of Casson nanofluid through convective condition. They computed the numerical solutions through Runge-Kutta Fehlberg. They found less velocity in the presence of magnetic field. Krishna and Reddy [8] explored the chemical reactive flow past a vertical plate by implementing heat source and magnetic field. Numerical solutions are computed for resulting dimensionless governing equations. Computational effects are discussed for speed, temperature and awareness profiles while numerical values of the skin friction, Nusselt number and Sherwood number has wide range of variety are tabulated for distinctive values of governing parameters controlling the flow gadget. Liu and Liu [9] presented characteristics of fractional Maxwell fluid deformed by wall having variable thickness. They showed the impact of various physical parameters on velocity graphical and explained elaborated. Reddy *et al.* [10] scrutinized the chemical radiative phenomenon in unsteady flow with slip conditions and magnetic field. They solved the system by Crake Nicholson scheme. They concluded that velocity decays as slip phenomenon enhances. Concentration was increased for higher constructive chemical rate parameter.

Ibrahim and Makinde [11] investigated the impact of double-stratified nanofluid flow on a boundary with heat transmission along a vertical surface and found that higher thermally stratified parameter resulted in lower temperature field. Mukhopadhyay [12] used magnetohydrodynamics (MHD) to analyze the boundary layer of an exponentially stretched thermal stratified medium. They found that higher stratified and magnetic parameters declined the velocity and temperature fields respectively. Thermal stratified phenomenon enhances heat exchange at the surface, as discussed by Sekhar [13]. Singh and Kumar [14] investigated MHD free convective in a micropolar while taking Joule heating, chemical processes, and heat generation into account. Hayat *et al*. [15] described the important properties of the heat transformation of dual-stratified flowing fluid distorted by a stretched surface. Kandasamy *et al.*

[16] investigated the effect of dual stratified phenomena on MHD nanofluid flow propagation in a vertical porous medium. It is established that enhancing the thermally stratified parameters resulted in decrement in the rate of heat transfer. Ahmad *et al*. [17] used a radioactive heat gradient and chemical modification to establish double stratification in Sutterby fluid flow. Bilal and Nazir [18] used nonlinear convection to examine the impact of stratification on non-Newtonian fluids. Reddappa *et al.* [19] investigated high thermal conductivity Jeffery fluid flow with a stratified over exponential stretched sheet. The phenomenon of double stratification and squeezing in Powell-Eyring fluid with generalized fluxes and inclined magnetic field was explored by Khan *et al.* [20].

Borrelli *et al.* [21] analyzed the features of orthogonal stagnation point in micropolar fluid flow with constant magnetic features by incorporating non-zero free stream velocity. Fluctuation increased in the flow due to growing free stream velocity. Fauzi *et al*. [22] scrutinized the characteristics of slip phenomenon in fluid flows located over the nonlinear shrinking sheet in the vicinity of stagnation. Merkin and Pop [23] examined the traits of fluid particles in the neighborhood of stagnation region by implementing Arrhenius kinetic energy. They used the exothermic reaction on the plate surface. Shafiq *et al.* [24] described the fluid's features in the vicinity of stagnation by incorporating Walter's B and deformed by Riga surface. They concluded that velocity enhances for dominant contribution Riga plate i.e., modified Hartmann number. Further, they noted that velocity of fluid particles grows as free stream velocity grows. Magnetized Carreau fluid in the surrounding of stagnation point over a stretchable surface with chemical reaction was discussed comprehensively by Khan *et al.* [25]. Dominant magnetic parameter resulted in decaying behavior of velocity field. Further, destructive chemical reaction resulted in lower concentration field. It is noticeable that boundary layer thickness increased for higher ratio parameter. Abbas *et al.* [26] presented the relation of stagnation point in three-dimensional flow of hybrid nanofluid by incorporating the slip factor at the plate's surface. According to authors, decaying behavior of velocity was noted for dominant slip factor whereas opposite trend was observed at the stagnation point for higher free stream velocity or stretching surface velocity. Khan *et al.* [27] discussed comprehensively the Carreau fluid traits at stagnation by implementing the Cattaneo-Christov model. They found that temperature diminished for higher Prandtl number and thermal relaxation parameter. The features of Oldroyd-B fluid were explored by Hayat *et al.* [28] by considering Brownian motion and

thermophoresis. Heat transportation was constraint to Cattaneo-Christov mode. Growing behavior of velocity was noted by higher free stream velocity and retardation parameter. Whereas, decaying behavior of temperature was achieved by higher thermal relaxation. Wahid *et al.* [29] elaborated the heat transportation in stagnation region of nanofluid flow over a shrinking sheet by implementing viscous dissipation and melting effect. Decrement was noted by the authors to enhance the melting phenomenon whereas growing behavior was observed for dominant Eckert number. Rehman *et al.* [30] emphasized the characteristics of stagnation with melting surface in Powell-Erying fluid with viscous dissipation and Joule heating. The flow was studied in the presence of thermal stratification. Temperature field was decayed gradually for higher melting and stratification.

Ramzan *et al.* [31] elaborated the features of Couple stress fluid by implementing Newtonian condition at the surface. They ignored the internal resistance of material for the conduction of heat. So temperature of fluid's particles was enhanced by higher conjugate parameter. Analysis of Burger fluid by taking variable thermal conductivity and modified heat models was described by Waqas *et al*. [32]. Decaying behavior of velocity was achieved by higher relaxation time whereas dominant retardation time resulted in opposite velocity trend. They noted that boundary layer thickness decreased in the case of higher relaxation parameter whereas it increased in the presence of higher retardation parameter. Skin friction was computed for the physical parameters and concluded that decrement occurred in the skin friction for growing values of retardation phenomenon. Hayat *et al.* [33] explored the characteristics of mixed convective phenomenon in Jeffrey fluid influenced by stretchable cylinder. Cylinder was presumed inclined with horizontal surface. Solutal and thermal stratifications were implemented to dig out the heat transportation. They concluded that velocity grows for higher mixed convective parameter whereas temperature and its boundary layer decayed for higher thermal stratified features of fluid. Similarly, decaying behavior of concentration was noted by the authors for dominant solutal stratified features. Hayat *et al.* [34] scrutinized the Carreau fluid in the stagnation region by considering nonlinear behavior of radiation which was generated by the heated sheet. Further, homogeneous and heterogeneous reactions were implemented within the fluid and at the surface of the sheet. Both the reactions were resulted in the opposite behavior of concentration of fluid particles. Temperature of the fluid particles was jumped continuously and gradually for higher intensity of thermal radiation parameter. Farooq *et al.* [35] studied

comprehensively the magnetic traits of squeezing phenomenon in Maxwell nanofluid. Lower plate was assumed stretched linearly in the horizontal direction whereas solutal and thermal stratifications were implemented to dig out thermal properties. Surface of the sheet was constrained to simultaneous effect of Fourier's and Newton's cooling laws. They emphasized that temperature was increased for growing Biot number and it was decayed for higher thermal stratified parameter. Squeezing parameter was resulted in the dominancy of fluid's particles which physically achieved from the movement of upper plate towards the lower one. The melting behavior of a surface through Powell-Eyring fluid was comprehensively studied by Javed *et al.* [36]. This study was accomplished with thermal stratified for the first with melting surface. Further, homogeneous and non-homogeneous reactions were implemented to find the best results of reactive fluids. For the first time, temperature decayed for higher stratification because fluid was considered heated whereas surface was cooled. Mahmel *et al.* [37] examined the properties of non-Newtonian fluid by incorporating nanoparticles through small pipes using both single- and two-phase flow models. Tizakast *et al*. [38] modeled the mixed convective flow due to temperature and concentration in any non-Newtonian fluid through rectangular cavity. Saini *et al.* [39] formulated the mathematical model for Creeping analysis in Jeffrey fluid through irregular porous medium. Malik *et al.* [40] explored the analysis of Falkner- Skan wedge flow in the Jeffrey fluid by assuming non-zero free stream velocity. Authors implemented nonlinear thermal stratifications within the fluid through variable temperature at sheet and surround fluid.

Farooq *et al.* [41] mentioned the impact of slip velocity at the drift of viscous fluid thru a porous medium in a permeable tube with a variable bulk waft charge. Soomro *et al.* [42] scrutinized the thermal and speed slip results on MHD combined convection drift of williamson nanofluid alongside a vertical surface: modified legendre wavelets approach. Nojoomizadeh *et al.* [43] investigated the permeability and porosity features at the slip pace and convective transportation rate of Fe3O4 or water nanofluid flow in a small channel. The lower half of this container was filled by a porous material. Ahmed *et al.* [44] analyzed the magnetohydrodynamic fluid floating and heat transportation influenced by shrinking sheet and having thermal jump at the surface of sheet. Khan *et al.* [45] modeled and computed the numerical answers of nanoliquid (graphene oxide, titanium oxide) flow by implementing second order slip. They also modeled the entropy for the current problem and discussed thoroughly with physical justifications. Rahmati *et al.*

[46] described the numerical computation to evaluate the non-Newtonian behavior of nanofluid in microchannels corresponding to slip phenomenon. Shah and Hussain [47] examined the slip effect in natural and force convective flows of UCM fluid saturated with porous material with heat flux modification. Yusuf *et al.* [48] targeted the irreversibility process of entropy in micropolar fluid film alongside an incline porous material with slip mechanism. Obalalu *et al.* [49] focused the effect of variable electric conductivity in Casson nanofluid flow with first and 2d-order slip situations embedded in an irregular porous material. Adigun *et al.* [50] implemented the stagnation factor in electrically conducting viscoelastic liquid located over the inclined cylinder's surface dipped in porous material. Further, they imposed the thermal and solutal stratifications on the fluid.

Ullah *et al.* [51] presented the magnetic impact of tangent hyperbolic fluid influenced by the linearly stretchable sheet. Further, sheet is presumed permeable to incorporate the suction or injection phenomenon. Solutions of arising nonlinear model are computed through shooting method. Impact of various parameters are graphically described corresponding to velocity and temperature fields. Decrement occurred in the velocity of fluid particles by enhancing the magnetic intensity. Jafar *et al.* [52] scrutinized the mathematical analysis of radiation phenomenon in nanofluid flow disturbed by the nonlinear stretching flat plate. Regular porous material was taken into account to dig out fluid features. Brownian phenomenon resulted in lower concentration field whereas thermophoresis increased the concentration of fluid. However, temperature declined due to higher radiation parameter. Fatunmbi and Adeniyan [53] analyzed the nonlinear behavior of radiation in incompressible and steady mircropolar fluid deformed by linearly stretchable surface. Variable thermal conductivity is inserted for thermal characteristics. Variable traits are imposed in the fluid flow modeling. Entropy generation was tackled through the second law of thermodynamics. Temperature was increased through higher conductivity parameter. Entropy generation enhanced for higher Eckert number. Authors noted that temperature was dominant in nonlinear radiation in comparison to linear radiation. Prasannakumara [54] explored the numerical simulation for the thermal transportation of Maxwell nanofluid deformable by linearly stretchable surface. Magnetic dipole phenomenon was introduced in the fluid to analyze the fluid flow. Khan *et al.* [55] examined the nanofluid features by slender stretchable sheet. Water is inserted as base fluid whereas two type nanoparticles are submerged into water. Single and Multi-wall Carbon nanotubes are used as

nanoparticles. Khan *et al.* [56] elaborated the deformation of fluid through stretching or shrinking sheet by incorporating linear solutal and thermal stratifications. Porosity condition is further imposed on the sheet material. Convective surface condition and velocity slip were implemented on the sheet's surface. Higher permeability enhanced the velocity. Temperature field decayed dramatically and gradually as thermal stratification increased. Similarly, concentration field decreased due to higher intensity of stratification via concentration. Khan *et al.* [57] executed the non-isothermal stretching surface effect on hybrid nanofluid with inertial and microstructure properties. The effects showed that the separation of boundary layer was averted by using higher depth of mass suction parameter whilst the contrary conduct was determined for the effects of the extent fraction of nanoparticles. Further, the friction trouble to start with uplifts and then declined due to suction for the primary solution, whilst decelerated for the second answer however the thermal transport and micro-rotation gradient adorned due to suction for every solution. The temperature augmented for both answer branches because of nanoparticles volume fraction while the micro-rotation and the rate reduced for the number one answer department even as uplift for the decreased solution department. Zainal *et al.* [58] described unsteady and incompressible stagnant flow in nanofluid flow. The deformation was produced by the exponential stretching sheet with the implementation of constant magnetic field in the vertical direction to fluid. The consequences also signified that the increment within the unsteady parameter conclusively increased the skin friction coefficient, and the thermal transfer indicated an upsurge attribution resulting from the inclusion of the magnetic parameter in the direction of an exponentially shrinking sheet. Also, the effects are evidenced via having twin solutions. Sarwar *et al.* [59] elaborated the Casson fluid flow with variable viscosity and bioconvection. Sheet was subjected to slip condition and stretched in horizontal direction. Mahbaleshwar *et al.* [60] scrutinized the mass transpiration in nanofluid through a stretching sheet with radiation emission. It was concluded by the authors that temperature field declined by the higher emission of radiation from the heated fluid.

The homotopy analysis method [61-70] is an effective analytical method for solving highly nonlinear differential equations. It is a generalization of the widely used homotopy perturbation method that gives a methodical approach for obtaining approximate results to nonlinear problems. The approach works by deforming a known solution to a simpler issue into a solution to a more complicated one. This strategy is very helpful for issues that cannot be solved using

typical analytical or numerical approaches. The core idea of HAM is to include a homotopy parameter, represented by **p**, which is a continuous variable ranging between 0 and 1. The nonlinear issue is turned into a family of analogous problems, with each member of the family representing a distinct value of. The issue is addressed first for **p** = 0, where it is reasonably straightforward, and then for **p** = 1, when it is more challenging. The answer for **p** = 0 is utilized as an initial estimate for the solution for **p** = 1, and the procedure is continued until a good solution is reached. The HAM's main benefit is that it offers a systematic method for obtaining approximate solutions to nonlinear problems. The technique is founded on the concept of transforming a known solution to a lesser issue into a solution to a more complicated one. This method is very beneficial for solving issues that cannot be addressed using standard analytical or numerical approaches. The fact that the HAM is a perturbation-free approach being one of its primary merits. In other words, unlike classic perturbation approaches, it does not need minor changes to the issue parameters to produce a solution. Because of this, the approach is especially beneficial for situations with high nonlinearities or singularities. Another benefit of the HAM is that it is simple to include into a computer Program. The approach is based on a straightforward iterative procedure that does not necessitate the use of sophisticated numerical methods. As a result, it is simple to use and accessible to a broad spectrum of people. It is not always feasible to use the HAM to find an acceptable solution, and the approach has several drawbacks. In some circumstances, the procedure might not lead to a solution or the result might not be precise enough for a given application. The approach may also depend on the initial approximation and homotopy parameter selection. The Homotopy Analysis Method, in conclusion, is a potent numerical method for resolving nonlinear differential equations. It offers a methodical approach to obtaining approximations for nonlinear problems and is especially helpful for issues that cannot be resolved by means of conventional analytical or numerical techniques. The approach is simple to use and has been used to solve a wide range.

CHAPTER 3

DEFINITION AND BASICS CONCEPT

This chapter describes some basic definitions, fundamental laws and some basics concepts to solve the nonlinear differential equations.

3.1 Fluid

Fluid is a substance which has ability of flowing. It has no definite shape of its own. It takes the shape or transform itself in that shape of container in which it contained or poured.
More precisely, fluid is defined as, "fluid is a material that cannot assist a tangential or shearing force in rest position and when apply such a shear stress the shape of the fluid will be continuously changed".
All liquids and gases exemplify the fluids. [72]

3.2 Fluid Mechanics

Fluid mechanics is the sub-category of continuum mechanics in which we study about fluids (liquids and gases), and also study of the effects of various forces and energy on them either at rest or in motion. In Fluid mechanics, we assume that fluid is a continuous medium (i.e., not made up of discrete molecules). As a result of the continuum assumption, each property of the fluid (i.e., ρ shows density, T shows temperature, V shows velocity, etc) is the continuous function of position and time. [73]

3.2.1 Fluid Statics

The study of the fluids in rest position is categorized as fluid statics. It is the primary subject which has some important classical results but this branch has less scope for the development of fluid mechanics. [74]

3.2.2 Fluid dynamics

The study of the moving fluids is categorized as fluid dynamics. Fluid dynamics is a theoretical and experimental subject in which results are analyzed by both physically and mathematically. Basic laws of Physics (i.e., Newtonian 2nd law of motion, energy and mass conservation laws) are used for the description of fluid's particle motion. [74]

3.3 Physical Properties of Fluid

3.3.1 Density

This is an intensive property of substance which is defined as mass contained in any unit volume. [72] Mathematically, it has the form:

$$\rho = \frac{M}{v}, \tag{3.1}$$

where M and V are mass and volume, respectively. The dimension of density is given by $\left[\frac{M}{L^3}\right]$.

3.3.2 Pressure

Pressure is the amount of force applied to a body's surface per unit area. Mathematically, this is written as follows:

$$p = \frac{F}{A}, \tag{3.2}$$

where F shows magnitude the force, A denotes cross-sectional area, and P is a pressure. [72]

3.3.3 Stress

Stress is a type of surface force defined as force per unit area. There are two types of stress. Tangent stress, also called as shear stress. [72]

3.3.4 Viscosity

The resistance experience by the viscous fluid during deformation called viscosity. Viscosity is the sign of internal friction and it plays a significant role in the thickness of fluid. [74] Mathematically, this can write as:

$$\text{Viscosity} = \frac{\text{Shearing stress}}{\text{Shearing rate change}}, \tag{3.3}$$

3.3.5 Kinematic viscosity

Kinematics viscosity relates to dynamic viscosity and density of fluid. In fluid mechanics, some problems required the inertial forces of fluid with the measurement of the viscosity. The inertial forces of fluids are highly dependent on the fluid's density. So, kinematic viscosity is attained by dividing the absolute viscosity of fluid by fluid's density. It gives us very useful information about the Newtonian fluids. Mathematically, it is expressed as follows:

$$\nu = \frac{u}{\rho}, \tag{3.4}$$

where is ρ fluid density and μ is dynamic viscosity. The dimension of kinematic viscosity is given by $\lfloor L^2T^{-1} \rfloor$. [74]

3.4 Flow

A continuous deformation of the material under very small shear stress is called flow phenomenon. [72]

3.5 Types of Fluid Flow

Fluid flow may be categorized into numerous categories depending on various characteristics. There are some of the general fluid flow classifications which are given as follows:

3.5.1 Rotational Flow

In this class of the fluid flow, particles of the fluid are flowing along streamlines and also rotate about their own axis. Through a small and light weight item in the flow, if the item spins, then this flow has a rotational behavior. [78]

3.5.2 Irrotational Flow

In this class of the fluid flow, particles of the fluid are flowing along streamlines but do not rotate about their own axis. We can observe irrotational flow in our bath tub draining. If we

place a light and small thing in that flow, it will go around the plug hole, but doesn't spin about itself. [78]

3.5.3 Compressible Flow

A fluid flow in which the ρ (density) of fluid particles varies from point to point or the fluid density does not remain same is known as compressible flow. [78]

3.5.4 Incompressible Flow

A fluid flow in which fluid particles density (ρ) does not vary from point to point or the ρ(density) of the fluid remains constant is known as incompressible flow. Generally, all the liquids are considered to have incompressible flow because it is quite difficult to compress the liquids. In hydraulic systems, liquids are used and treated as incompressible flows. In fans and blowers, the flow of gases is treated as compressible flows. [78]

3.5.5 Laminar Flow

The fluid flow in which the movement of the fluid particles or molecules is in a very order manner and having smooth layers of fluid is known as laminar flow. [78]

3.5.6 Turbulent Flow

In turbulent flow, due to the rapid change in pressure and velocity with respect to space and time, the fluid flow does not travel in smooth layers and there is a significant mixing of layers. As a result, fluid particles don't move in highly order manner and cross the path of other particles.[78]

3.5.7 Steady Flow

In this class of fluid flow, the fluid characteristics (velocity, pressure, density, etc.) at every point in the flow remains unchanged with time. In steady flow, fluid properties may be the function of spatial coordinates. [78]

3.5.8 Unsteady Flow

In this class of fluid flow, the fluid characteristics (velocity, pressure, density, etc) at every point in the flow changes with time. In unsteady flow, fluid properties may or may not the function of spatial coordinates. [78]

3.5.9 Internal Flow

Internal flow system is defined as the movement of the fluid particles within the closed surfaces. Examples include flow through pipes, ducts, or open channels. [72]

3.5.10 External Flow

Flow in which the fluid movement don't need any specific boundaries. Common examples include moving ships in ocean, water flow through the nozzle of fire extinguisher and fluid flow in rainy weather. [72]

Internal and external flow systems may be laminar, turbulent, compressible or incompressible.

3.6 Types of Fluids

Fluids are classified into the following categories:

3.6.1 Real Fluid

As we know that the density of actual fluid can change result of pressure changes. So, every fluid we see around us is a true fluid such as water, fuel, oil, honey and so on. Flow phenomenon of real fluid can be discussed with help of Navier Stokes equation which are partial differential equation (PDEs) with high non linearity. [75]

3.6.2 Ideal Fluid

Ideal fluids can’t be compressed. This indicates that pressure has no effect on the fluid s density or volume. It is impossible to give an example of an ideal fluid because they only exist in theory and not in reality. The flow of non-viscous fluids are discussed with help of Euler equation. Fluid dynamics is governed by a set of quasilinear partial differential equations known as the Euler equations, which control adiabatic and inviscid flow. They take their name from Leonhard Euler. They are particularly related to Navier-Stokes equations with zero heat conductivity and zero viscosity. [75]

3.6.3 Newtonian Fluid

Newtonian fluids follow Newton's law of viscosity, which determines the relationship between a fluid s shear stress and shear rate when subjected to mechanical stress, and the viscosity of a Newtonian fluid is independent of the shear rate. Air and water are examples of Newtonian fluids. It addresses that the shear/tangential stress among two consecutive fluid's layers is directly proportional to gradients of velocity among the two layers. The stress to strain ratio is constant at described temperature and pressure and is defined as the viscosity or coefficient of viscosity. Mathematically, we can write as follows:

$$\tau = \mu \frac{du}{\mathrm{d}\, y}, \tag{3.5}$$

where, μ represents dynamic viscosity, $\frac{du}{\mathrm{d}\, y}$ shows the rate of deformation and τ depicts shear stress. [75]

3.6.4 Non-Newtonian Fluid

There are some non-Newtonian fluids are those in which the strain rate is not proportional to the stress, as well as their higher powers. Toothpaste, cosmetics, and butter are examples of non-Newtonian Fluids. Mathematically, it is written as follows:

$$\tau = \mu \left(\frac{du}{\mathrm{d}\, y}\right)^n, \tag{3.6}$$

where $n \neq 1$, n is behavior index for flow and $\frac{du}{\mathrm{d}\, y}$ represents shear rate. [75]

3.7 Thermal Energy Transport Mechanism

Temperature difference is the basic cause for the transfer of heat from one body to another. Heat always flows from the region of hotter body to the region of colder body and this process is continued until the state of thermal equilibrium is attained. Depending upon the nature of the material under consideration, heat flows from one body to another by different processes.

3.7.1 Conduction

Conduction is the process in which thermal energy transport in direct physical contact of items and molecules. Conduction is the process in which thermal energy is transferred from the more energetic particles in a material to the other particles having lower energy, as a consequence of the interaction between particles. Conduction process can exist in solids, liquids, and gases (when liquids and gases are in rest position). In liquids and gases, the conduction occurs by means of molecular collision/ diffusion during their motion. In solids thermal energy transported due to the combine effect of vibration of molecules in lattice (in non-conductors) and by free electrons (in conductors).

To find the heat transfer rate by conduction, we use the "Fourier's law of heat conduction". Fourier law of heat conduction is applied to study the conduction process and mathematically, expressed as:

$$\tilde{q} = k\nabla\tilde{T}, \tag{3.7}$$

where $\tilde{q}$ is flux of heat waves and $\nabla\tilde{T}$ is thermal gradient. [76]

3.7.2 Convection

Convection needs a medium, just like conduction does, unlike radiation. Convection, on the other hand, involves the heated fluid actually moving, whereas conduction involves the heat being transmitted from one molecule to other. Cold air in its path is either removed are displayed as its follows. Convection mode of heat transfer illustrates the heat transfer process in which thermal energy transfers between a solid surface and the object moving i.e., fluid (liquid/gas), and it implies both impacts of conduction and fluid motion. If bulk fluid motion is absent then transportation of heat among adjacent fluid and a solid surface is taken by pure conduction. If the fluid motion is faster then there is higher convection heat transfer. The rate of convection heat transfer can be calculated by Newton's law of cooling, its mathematical form is given below: Convection current is the term use to describe the flow of hot fluids in this scenario. Mathematically, it is expressed as:

$$\tilde{Q} = hA\left(\tilde{T}_{hot} - \tilde{T}_{cold}\right), \tag{3.8}$$

where, $\tilde{Q}$ represents heat flux, h represents heat transfer coefficient, A refer area. Convection is further categorized into the follow three types: i.e., Natural convection exists due to difference in temperatures which affect the density and thus involve buoyancy of the fluid. High density elements will sit on the bottom of the surface while having light density elements rise above leading to bulk fluid movement. Natural convection phenomenon arises only in gravitational field. When the density difference is created by some external means due to which movement of fluid takes place then it is termed as forced convection. It is also called heat advection, the movement of the fluid encountered as a result of some external force and the source of this external force may be a fan or a pump. For the mixing of different types of substances into each other the utilization of forced convection is convenient. An oven works by forced convection, a fan which rapidly circulates and heat the food faster than without the fan. The effect of both forced convection and natural convection in a phenomenon is called mixed convection. [76]

3.7.3 Radiation

Electromagnetic waves are the carrier of thermal energy, this process is called radiation. In the radiation mode of heat transfer, thermal energy is transferred by radiation emitted by a body having temperature above absolute zero. Radiations are emitted from a material in the form of electromagnetic waves due to the changing in the electronic configuration of atoms. There is no need of any intervening medium for the transfer of heat by radiations. Stefan-boltzmann law is used to find the max rate of radiations emitted by surface. [76]

3.8 Thermal Conductivity

Thermal conductivity is the property of the matter and may be stated as; "the rate of heat transfer through a unit thickness of a material per unit area, per unit temperature difference". Thermal conductivity is a material's ability to conduct heat. Different materials have different thermal conductivity. A material which has high value of thermal conductivity shows a good conductor of heat while a material having low value of heat conductivity shows the poor conductor of heat or an insulator. The S.I unit of thermal conductivity is kg.m/s³.K (W/m) and dimension is $[MLT^{-3}\theta^{-1}]$. [76]

3.9 Thermal Diffusivity

The thermal diffusivity determines how quickly heat conducts through a substance. Thermal diffusivity is an important term in heat transport. The rate at which temperature travels over a substance is referred to as thermal diffusivity. Mathematically can be defined as:

$$\alpha = \frac{k}{\rho C_p}, \tag{3.8a}$$

where thermal diffusivity is represented by α, k shows the thermal conductivity, c_p represents specific heat capacity. [77]

3.10 Permeability

A fluid equation was created in 1856 by Darcy (also known as Darcy), and it has since because one of fundamental mathematical tool used by petroleum engineer. He looked at how water passes through a sand filter to purify it. After that investigation, he proves that his formulation can applied to other type of viscous fluids. Mathematically, Darcy observation can be express as:

$$\Omega = -kA\frac{p_2 - P_1}{\mu_L}, \tag{3.9}$$

where, Ω is permeability parameter, μ is dynamic viscosity, L is characteristic length and k is permeability of porous medium.

A porous medium is a substance which has voids/pores or a porous matrix. These pores may or may not be of the same sizes and shapes. The porous matrix is usually solid while the pores are filled with a fluid i.e., liquid or gas. According to this definition, many materials are come to this category, e.g., body tissues, sand, wood, soil, and sponges, etc.

Let volume of the pores/voids be V_v. When the fluid flows through the pores/voids of a porous medium V, the walls of these pores/voids form small tunnels through which the flow of fluid is possible. A study in which the fluid motion is in a porous medium on pores scale is known as microscopic scale. The study of microscopic scale is complicated and unrealistic because porous media has the complex micro-geometry. To avoid this complexity, we can take macroscopic continuum assumption.

3.11 Magnetohydrodynamic (MHD)

The study of mutual interaction of magnetic field in an electrically conducting fluid is demonstrated as magnetohydrodynamic. As electric current induced in the fluid which consequently modify the field due to its motion and simultaneously mechanical forces are produced which also modify the motion. The Maxwell equations that characterize the magnetohydrodynamics impacts are:

$$\nabla . E = \rho e / \varepsilon_0, \tag{3.10}$$

$$\nabla . B = 0, \tag{3.11}$$

$$\nabla \times E = -\partial B / \partial t, \tag{3.12}$$

$$\nabla \times B = \mu_0 J + \mu_0 \, \varepsilon_0 \, \partial E / \partial t. \tag{3.13}$$

Here, J depicts density of current, ε_0 represents electrical permittivity, B depicts the magnetic field, E shows the electric field and μ_0 demonstrates magnetic permeability. [79]

3.12 Electric Field

An electric field can be defined as the electric force per unit charge. According to mathematics, the electric field is characterized as a vector field that may be associated to any place in space and reflects the force per unit charge delivered to a point charge that is at rest at that position.

3.13 Resistive Heating

Joule heating represents the loss of energy flowing to a magnetic field in an electrically conducting fluid. According to Ohm's generalized law,

$$\boldsymbol{J} = \sigma[\boldsymbol{V}\,\boldsymbol{B} + \boldsymbol{E}], \tag{3.14}$$

where, σ denotes electrically conducting, $\boldsymbol{E}$ shows electric field, current density displayed $\boldsymbol{J}$, $\boldsymbol{V}$ expressed velocity and $\boldsymbol{B}$ shows magnetic field.

3.14 Viscous Dissipation

Viscous dissipation shows the energy is wastage in form of heat due to resistance between fluid particles during flow.

3.15 Flow over Stretching Sheet

Two forces of equal magnitude but opposite directions are applied to a sheet, the midpoint remains constant or the ability of a sheet to return to its original shape when subjected to shear stress is known as a stretching sheet. The flow of a viscous fluid over a stretched sheet has a variety of useful applications, including sheet polymer extraction and plastic sheet drawing. The melt for these sheets is created during manufacture from silt and then stretched to the necessary thickness. The required qualities of the end product are exclusively dictated by the stretching rate and the pace of cooling in the process.

3.16 Dimensionless number

3.16.1 Reynold Numbers

Reynolds number is a non-dimensional quantity. Reynolds number addresses the relation between inertial and viscous forces and is also useful in predicting flow behavior either turbulent or laminar". Mathematical form of Reynolds number is given below:

$$Re = \frac{(Inertial\ forces)}{(Viscous\ forces)} = ((\rho VL)/\mu), \tag{3.15}$$

$$\Rightarrow Re = LV/\upsilon. \tag{3.16}$$

In the above equation, V represents velocity of the fluid flow, L denotes characteristic length, υ demonstrates the kinematic viscosity. If the inertial forces are dominated than the viscous forces then the flow is demonstrated as turbulent. Higher Reynolds number (Re) specifies turbulent flow. If the viscous effects are dominated then the behavior of the flow will be laminar. [82]

3.16.2 Nusselt Number

The Nusselt number is a dimensionless quantity that represents the ratio of convective to conductive heat transmission. Nusselt number is a representation of non-dimensional gradient of temperature in the fluid at the interphase among the fluid and the solid. In heat transfer, with in a

fluid at a boundary, the Nusselt number (N_u) is stated as; "the ratio of the convective heat transfer to the conduction heat transfer normal (across) to the boundary. Convection mode of heat transfer contains both diffusion and advection. Nusselt number's mathematical expression is:

$$N_u = \frac{hL}{k}, \tag{3.17}$$

where, k depicts thermal conductivity and L revealed the characteristic length, h is the heat transfer coefficient, N_u denotes the Nusselt number.

3.16.3 Prandtl Number

The dimensionless number was given the name Prandtl number by German scientist Ludwing Prandtl. It is the ratio of heat diffusivity to momentum diffusivity.

$$P_r = \frac{\nu}{\alpha}, \tag{3.18}$$

where, α reflects thermal diffusivity and ν displayed momentum diffusivity.

3.16.4 Hartmann Number

Drag force that results from magnetic and viscous forces is discussed under this dimensionless parameter. Hartman number relates electromagnetic and viscous forces.

$$M = \frac{magnetic\ force}{viscous\ force}, \tag{3.19}$$

3.16.5 Eckert Number

The Eckert number is a non-dimensional number used in fluid mechanics. It characterizes heat transfer dissipation by expressing the relationship between a flow's kinematic potential and the boundary layer entropy. Eckert number is a non-dimensional parameter. This number gives the measurement of the kinetic energy of the fluid flow relative to the enthalpy (temperature difference) difference across the thermal boundary layer. It is also used for the characterizing heat dissipation in high-speed flow for which the viscous dissipation is significant. [72]

3.16.6 Schmidt Number

The Schmidt numbers is a non-dimensional number that is affected by the momentum to mass diffusivity ratio. It can be used to solve the mass transfer issue. Or it relates the momentum and mass diffusivities. Physically, it is the measure of the relative efficiency of diffusion due to momentum and mass transport i.e., relative thickness of momentum and solutal boundary layers.

3.16.7 Sherwood Number

The ratio of convective mass transfer to diffusion in slab of thickness L [83]. Mathematically,

$$Sh = \frac{hL}{D}, \tag{3.20}$$

where, L represents the length, h is the convective mass transfer and D denotes mass diffusivity.

3.16.8 Skin Friction

Drag force arises from the movement of the fluid at the surface is demonstrated as skin friction coefficient. Whenever fluid moves over the body then drag force is produced due to shear forces acting upon the surface of the body. Mathematically it is defined as:

$$C_f = \frac{2\tau_w}{\rho U^2}, \tag{3.21}$$

In above relation τ_w represents the shear stress at the surface, U stands for velocity and ρ denotes the fluid density. [81]

3.17 Stratification

A fluid phenomenon caused by the formation of layers in response to changes in temperature, concentration, or the presence of several fluids with varying densities.

3.18 Slip phenomena

Slip problem is characterized by the difference in velocity between fluid particles and a surface. Blood flow and the use of mercury in thermometers are examples of slip flow. It is useful in

prosthetic heart coating, accurate information analysis in ducts and cylinders, surface sensitivity reduction, renewable power savings, and other applications.

3.19 Reynolds Transport Theorem

According to the Reynolds transport theorem, the rate of change of a systems extensive property with respect to time is equal to the product of the rate of change of a control volumes property per unit time and the rate of the property. The Reynolds theorem is a three-dimensional generalization of the Leibniz integral rule. The name is derived from Osborne Reynolds. The fundamental purpose of the Reynold transport theorem is to assist drive conservation principles such as momentum conservation, linear momentum conservation, mass conservation, kinetic energy conservation.

3.20 Boundary Layer Theory

L. Prandtl (1904) proposed the fundamental concept of the boundary layer, which denotes the boundary layer as the zone where flow transitions from zero velocity at the wall to a maximum in the ow s mainstream. A velocity boundary layer forms when fluid flows over a surface, and a thermal boundary layer forms if the bulk and surface temperatures differ. When an object passes through a fluid or a fluid passes through an object, the molecules in the fluid surrounding the object are disrupted and flow all around object. Between the fluid particles and the object, aerodynamic forces are created. The amount of these forces is determined by the form of the item, its speed, the mass of the fluid passing through it, and two other significant characteristics of the fluid are viscosity and compressibility. The properties of flow within the layer at border are crucial for many aerodynamic difficulties, including high-speed heat transfer and skin friction created in an object.

3.20.1 Velocity Boundary Layer

The velocity boundary layer is the zone defined by the velocity gradient in which the flow velocity is distributed throughout the various fluid layers. Consider the flow of a fluid across a fixed surface. Regardless of flow behavior, the fluid particles adhere to the surface because of the viscous effects, and the velocity of the fluid contacting the solid surfaces are brought to a halt

by shear stress. This shearing force also causes a velocity distribution in the flow s normal direction.

3.20.2 Thermal Boundary Layer

The thermal layer at boundary is the region of fluid flow determined by the difference in temperature caused by thermal energy transfer between the surrounding layers. When a fluid at temperature T flows across a at plate at temperature T_w, the fluid particles at the boundary layer that comes into direct touch with the surface achieves thermal equilibrium. Conduction is responsible for the energy flow at this point. However, within neighboring fluid layers, conduction and diffusion enable exchange of energy to generate a temperature gradient, which has a similar property to the velocity difference near the boundary layer.

3.20.3 Concentration Boundary Layer

The concentration boundary layer refers to the area where the difference in concentration between the plate and the freestream has reached 99% of the difference in concentration between both the plate and the freestream. When two or more fluids are joined, mass transfer is caused by both convection currents and concentration changes. Heat transfer by conduction is treated similarly to related mass transport via diffusion.

3.21 Displacement Thickness

Displacement thickness is characterized as the distance measured perpendicular to the solid surfaces boundary by which the solid surfaces border should be displaced to compensate for the decline in flow rate induced by boundary layer growth.

3.22 Momentum Thickness

Momentum thickness is described as the distance measured normal to the solid object border by which the boundary should be shifted to compensate for the loss in owing fluid momentum produced by boundary layer development.

3.23 Energy Thickness

The energy thickness is the thickness of flow travelling at free stream velocity and containing kinetic energy equal to the kinetic energy deficit generated by boundary layer development.

3.24 Thermal Stratification

We know that oceans, rivers, and lakes directly receive sunlight from the sun. This direct sunlight effects the water layers in the ocean, lakes, and rivers. Consequently, there becomes significantly clear layers of water of different temperatures. The process of formation of these layers is called thermal stratification. Mainly, there are two distinct layers of water of different temperatures. On the top surface (upper layer of the reservoir), the layer will be warmer and is called Epilimnion. At the bottom of the ocean, the layer will be colder and is called Hypolimnion. Each layer has a specific uniform temperature relative to the other layers. Further both layers are separated by a region where the temperature has rapid change and this region is called Metalimnion or Thermocline. Since these layers of different temperatures have different densities. Low dense water will be at the top surface of the oceans. Denser water will be at the bottom of oceans.

3.25 No-Slip Boundary Condition

If the velocity of the fluid layer which is in contact to the surface is same to the velocity of the surface, this phenomenon is known as no-slip flow. Or when the fluid flow is enclosed by a solid surface, then the molecular collisions occur between fluid particles and surface in order to achieve energy equilibrium and momentum of the surface. i.e.; this phenomenon is known as no-slip condition.

3.26 Slip Boundary Condition

In the slip boundary condition, the velocity of the surface and the fluid layer are not same. Mercury is a good example for the understanding of slip flow. Whenever the no-slip boundary condition cannot be applied, slip conditions to be considered. or if relative velocity of the plate and the fluid particles is different, then such phenomenon is demonstrated as slip condition. Mercury used in thermometer is one of the best examples of slip phenomenon.

3.27 Governing Equations

3.27.1 Mass Conservation Law

It states that the total mass of the system is conserved in closed system. Mathematically

$$\left(\frac{\partial}{\partial t}+\mathbf{V}.\nabla\right)\rho+\rho\nabla.\mathbf{V}=0, \tag{3.22}$$

or

$$\frac{\partial\rho}{\partial t}+(\mathbf{V}.\nabla)\rho+\rho\nabla.\mathbf{V}=0, \tag{3.23}$$

or

$$\frac{\partial\rho}{\partial t}+\nabla.(\rho\mathbf{V})=0. \tag{3.24}$$

It is also named as continuity equation. Here ρ stands for the density of the fluid and $\mathbf{V}$ depicts the velocity profile. In steady state flow above equation takes the following form

$$\nabla.(\rho\mathbf{V})=0, \tag{3.24}$$

and for incompressible fluid flow the above expression takes the following form [80]

$$\nabla.\mathbf{V}=0. \tag{3.25}$$

3.27.2 Momentum Conservation Law

It describes that momentum remains constant for any system. It is derived from Newton's second law.

$$\rho\frac{D\mathbf{V}}{Dt}=\nabla.\boldsymbol{\tau}+\rho\mathbf{b}, \tag{3.26}$$

$$\tau=-PI+\mu A_1, \tag{3.27}$$

where $\mathbf{A}_1$ is first Revilin Erickson tensor.

$$\mathbf{A}_1=\text{grad}\,\mathbf{V}+(\text{grad}\,\mathbf{V})^T, \tag{3.28}$$

$$grad\mathbf{V}=\begin{bmatrix}\frac{\partial u}{\partial x} & \frac{\partial u}{\partial y} & \frac{\partial u}{\partial z}\\ \frac{\partial v}{\partial x} & \frac{\partial v}{\partial y} & \frac{\partial v}{\partial z}\\ \frac{\partial w}{\partial x} & \frac{\partial w}{\partial y} & \frac{\partial w}{\partial z}\end{bmatrix}. \tag{3.29}$$

Inertial forces are represented by $\rho \frac{D\mathbf{V}}{Dt}$, surface forces by $\nabla.\boldsymbol{\tau}$ and body forces by $\rho\mathbf{b}$ respectively. Pressure is denoted by P , $\mathbf{I}$ represents the identity tensor, $\frac{D}{Dt}$ shows the material time derivative while $\mathbf{b}$ represents body force per unit density. [80]

3.27.3 Energy Conservation Law

This law reflects that total energy of the system is conserved. It is computed from Ist law of thermodynamics. Mathematically

$$\rho_f C_p \frac{DT}{Dt} = \boldsymbol{\tau}.\mathbf{L} + k\nabla^2 T. \tag{3.30}$$

where ρ_f stands for base fluid density, C_p represents the specific heat of the base fluid, T stands for temperature, $\boldsymbol{\tau}$ represents the stress tensor, $\mathbf{L}$ stands for rate of strain tensor, k is the thermal conductivity. [76]

3.28 Solution Methodology

HAM technique is one of the best and simplest technique for obtaining convergent series solution for weakly as well as strongly non-linear differential equations. This method based on the concept of homotopy in topology. Two functions are homotopic if one function deforms continuously into other function, e.g. $f_1(x)$ and $f_2(x)$ are two functions and F^* is a continuous mapping, then

$$F^* : X \times [0,1] \to Y, \tag{3.31}$$

such that

$$F^*(x,0) = f_1(x), \tag{3.32}$$

and $F^*(x,1) = f_2(x)$. Laio [61] in 1992 used the homotopic technique for obtaining convergent series solution. HAM distinguishes itself from other techniques in the following ways:

1. It is independent of small/large parameter.
2. Convergent solution is insured.
3. Freedom for the choice of base functions and linear operators.

Consider a non-linear differential equation

$$\mathbf{N}[u(x)] = 0, \tag{3.33}$$

where $\mathbf{N}$ represents non-linear operator, and $u(x)$ is the unknown function.

Using parameter $p \in [0,1]$, a system of equations is constructed.

$$(1-p)\mathbf{L}\left[\widehat{u}(x;p)-u_0(x;p)\right]=p\hbar\mathbf{N}\widehat{u}(x;p), \tag{3.34}$$

where $\mathbf{L}$ is linear operator, p is embedding parameter and $\hbar$ is convergence parameter. By putting value of p from 0 to 1, unknown function gets the value from $u_0(x)$ to $u(x)$.

$$\widehat{u}(x;p)=u_0(x)+\sum_{k=0}^{m-1}u_m(x)\,p^m, \qquad u_m(x)=\frac{1}{m!}\frac{\partial^m\widehat{u}(x;p)}{\partial x^m}|_{p=0} \tag{3.35}$$

For $p=1$ we get,

$$u(x)=u_0(x)+\sum_{m=1}^{\infty}u_m(x). \tag{3.36}$$

For m^{th} order problems we have,

$$\mathbf{L}_u\left[u_m(\eta)-\chi_m u_{m-1}(\eta)\right]=\hbar_u\mathbf{R}_m^u(\eta), \tag{3.37}$$

$$\mathbf{R}_m^u(\eta)=\frac{1}{(m-1)!}\frac{\partial^m\mathbf{N}_u\widehat{u}(x;p)}{\partial x^m}|_{p=0}, \tag{3.38}$$

$$\chi_m=\begin{cases}0, & m\le 1\\ 1, & m>1\end{cases}. \tag{3.39}$$

CHAPTER 4

ANALYSIS OF MAGNETOHYDRODYNAMIC STAGNATION POINT FLOW WITH POROUS MATERIAL

4.1 Introduction

This chapter comprises the entire study of the incompressible, electrically conducting stagnation point flow of fluid having viscosity on a stretching sheet that is linearly deformed [71]. The fluid flow is subjected to a magnetic field in the perpendicular direction. Heat sink and source are features of heat transport due to the assumed effects of porous media. The obtained model equations are transformed into a non-dimensional form. The use of the homotopy method is helpful for convergent series solutions. Numerous distinct dimensionless parameters are used to investigate the characteristics of the temperature and velocity profiles. As a conclusion, the temperature and velocity profiles show decaying behavior for higher Prandtl numbers and magnetic field parameters, as well as they show an increasing trend for the blowing parameter, respectively. The Nusselt number and frictional drag are mathematically and graphically represented. The mathematical and graphical behavior of the Nusselt number and frictional drag are explored using a various emerging parameter.

4.2 Problem statement

This discussion examines the flow of a two-dimensional, steady, electrically conducting having incompressible behavior of viscous fluid moving across a horizontally heated, stretched linear sheet. The sheet is horizontally oriented and fluid flow is considered to take place through the porous material with hole of comparable sized. For the interpretation of stagnation point free stream flow, velocity components are taken to be non-zero. Heat absorption/generation coefficient is also considered in order to investigate the heat transportation properties. Wall temperature of heated plate is assumed to be changeable as well as greater than the temperature

of surrounding (see Fig. 4.1). The governing equation, after applying boundary layer model are as follows:

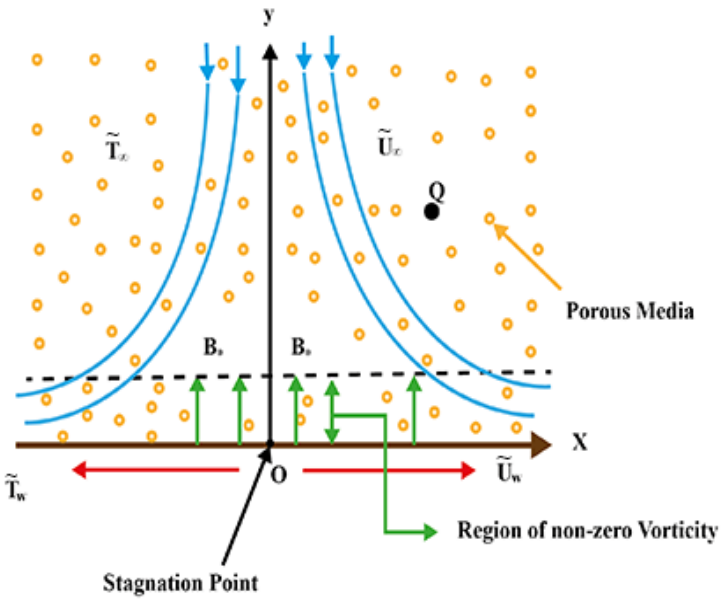

Fig. 4.1: Flow Model

$$\frac{\partial \tilde{u}}{\partial x} + \frac{\partial \tilde{v}}{\partial y} = 0, \tag{4.1}$$

$$\tilde{u}\frac{\partial \tilde{u}}{\partial x} + \tilde{v}\frac{\partial \tilde{v}}{\partial y} = \tilde{U}_\infty \frac{d\tilde{U}_\infty}{dx} + \nu\frac{\partial^2 \tilde{u}}{\partial y^2} + \frac{\sigma {B_0}^2}{\rho}\left(\tilde{U}_\infty - \tilde{u}\right) - \frac{\nu}{K}\left(\tilde{u} - \tilde{U}_\infty\right), \tag{4.2}$$

$$\tilde{u}\frac{\partial \tilde{T}}{\partial x} + \tilde{v}\frac{\partial \tilde{T}}{\partial y} = \alpha\frac{\partial^2 \tilde{T}}{\partial y^2} + \frac{Q}{\rho c_p}\left(\tilde{T} - \tilde{T}_\infty\right). \tag{4.3}$$

The boundary condition are as follows:

$$\tilde{u} = \tilde{U}_w(x) = ax, \quad \tilde{T} = \tilde{T}_w(x) = \tilde{T}_\infty(x) + cx^n, \text{ at } \tilde{\eta} = 0, \tag{4.4}$$

$$\tilde{u} = \tilde{U}_\infty(x) = bx, \quad \tilde{T} = \tilde{T}_\infty(x) = 0, \text{ as } \tilde{\eta} \to \infty. \tag{4.5}$$

Here, $\tilde{u}$ and $\tilde{v}$ depicts velocity components which displays along the directions of x and y respectively, σ displays electrical conductivity, specific thermal conductivity is depicted by c_p, the strength of magnetic field is denoted by B_0, constant permeability of porous media depicts K, and $\tilde{U}_\infty(x)$ indicates by free stream velocity, ρ shows density, k corresponds to thermal conductivity, Thermal diffusivity is symbolized by the symbol α, $\tilde{U}_w(x)$ demonstrates stretching velocity, Q denotes heat absorption ($Q > 0$) or generation ($Q < 0$).

4.3 Transformations

Transformation for the current flow of fluid problem is shown as:

$$\tilde{f}\,(\tilde{\eta}) = \frac{\psi}{(av)^{\frac{1}{2}}x}\,,\ \tilde{\theta}(\tilde{\eta}) = \frac{(\tilde{T}-\tilde{T}_\infty)}{(\tilde{T}_w-\tilde{T}_\infty)}\,,\tilde{\eta} = \left(\frac{a}{\nu}\right)^{\frac{1}{2}} y,$$
$$\tilde{u} = ax\,\tilde{f}'(\tilde{\eta}),\ \ \tilde{v} = -(av)^{\frac{1}{2}}\tilde{f}\,(\tilde{\eta}). \tag{4.6}$$

The continuity equation disappears after applying the above transformation, however the following governing equation stayed:

$$\tilde{f}''' + \tilde{f}\tilde{f}'' - \tilde{f}'^2 + M\left(\epsilon - \tilde{f}'\right) - \Omega\left(\epsilon - \tilde{f}'\right) = 0, \tag{4.7}$$

$$\frac{1}{P_r}\tilde{\theta}'' + \tilde{f}\,\tilde{\theta}' - n\,\tilde{f}'\tilde{\theta} + \gamma\tilde{\theta} = 0. \tag{4.8}$$

The following are the appropriate boundary condition,

$$\tilde{f}(0) = s, \tilde{f}'(0) = 1, \tilde{f}'(\infty) \to \epsilon,$$
$$\tilde{\theta}(0) = 1, \tilde{\theta}(\infty) = 0. \tag{4.9}$$

Here, the permeability parameter denoted by Ω, the heat absorption and generation coefficient are elaborated by γ, ϵ shows the ratio between velocity parameter, Prandtl number represented by P_r and M reflects the magnetic parameter, explained as follows:

$$\Omega = \frac{\nu}{ak}, \qquad \gamma = \frac{\mathrm{Q}}{\mathrm{a}\rho\mathrm{c_p}}, \qquad \epsilon = \frac{b}{a}, \quad P_r = \frac{\nu\mathrm{M} = \frac{\sigma {B_0}^2}{a\rho}}{\alpha}$$

Some physically relevant values of importance are presented as local Nusselt number and skin friction coefficient,

$$N\tilde{u}_x = \frac{xq_w}{k(\tilde{T}_w - \tilde{T}_\infty)}, \qquad C_{\tilde{f}} = \frac{\tau_w}{\rho {\tilde{U}_w}^2},$$

where,

$$\tau_w = \mu\left(\frac{\partial\tilde{u}}{\partial y}\right)_{y=0}, \qquad q_w = -k\left(\frac{\partial\tilde{T}}{\partial y}\right)_{y=0}.$$

The local heat flow is shown by q_w, while the wall shear stress is shown by τ_w.

The following are examples of quantities in non-dimensional representation:

$$Re_x^{\frac{1}{2}}C_{\tilde{f}} = \tilde{f}''(0), \qquad Re_x^{\frac{1}{2}}N\tilde{u}_x = -\,\tilde{\theta}'(0), \tag{4.10}$$

where the regional Reynold number is given by $Re_x = \frac{\tilde{U}_w(x)\,x}{\nu}$.

4.4 Homotopic Solutions

The following are the initial guesses for the momentum and energy equation:

$$\widetilde{f_0}(\tilde{\eta}) = \varepsilon x + s + \left(1 - e^{-\tilde{\eta}}\right) - \varepsilon(1 - e^{-\tilde{\eta}}), \tag{4.11}$$

$$\tilde{\theta}_0(\tilde{\eta}) = e^{-\tilde{\eta}}. \tag{4.12}$$

The auxiliary operators $\tilde{f}$and $\tilde{\theta}$ have a linear expression as:

$$L_{\tilde{f}} = \frac{d^3\tilde{f}}{d\tilde{\eta}^3} - \frac{d\tilde{f}}{d\tilde{\eta}}, \tag{4.13}$$

$$L_{\tilde{\theta}} = \frac{d^2\tilde{\theta}}{d\tilde{\eta}^2} - \tilde{\theta}. \tag{4.14}$$

The following properties are satisfying as follows:

$$L_{\tilde{f}}(A + Be^{-\tilde{\eta}} + Ce^{-\tilde{\eta}}), \tag{4.15}$$

$$L_{\tilde{\theta}}\left(De^{-\tilde{\eta}} + Ee^{-\tilde{\eta}}\right). \tag{4.16}$$

4.4.1 Zeroth- Order

The modified equations for task of the zeroth order are written as:

$$(1-p)L_{\tilde{f}}\left[\tilde{f}(\tilde{\eta},p) - \tilde{f}_0(\tilde{\eta})\right] = ph_{\tilde{f}}N_{\tilde{f}}[\tilde{f}(\tilde{\eta},p)], \tag{4.17}$$

$$(1-p)L_{\tilde{\theta}}\left[\tilde{\theta}(\tilde{\eta},p) - \tilde{\theta}_0(\tilde{\eta})\right] = ph_{\tilde{\theta}}N_{\tilde{\theta}}[\tilde{f}(\tilde{\eta},p), \tilde{\theta}(\tilde{\eta},p)], \tag{4.18}$$

$$\tilde{f}(0,p) = s, \quad \widetilde{f}'(0,p) = 1, \quad \tilde{f}'(\infty,p) \to \varepsilon, \tag{4.19}$$

$$\tilde{\theta}(0,p) = 1, \quad \tilde{\theta}(\infty,p) \to 0, \tag{4.20}$$

where the non-linear operators $N_{\tilde{f}}$ and $N_{\tilde{\theta},}$ are defined as follows:

$$N_{\tilde{f}}\left[\tilde{f}(\tilde{\eta},p)\right] = \begin{matrix} \frac{\partial^3\tilde{f}(\tilde{\eta},p)}{\partial\tilde{\eta}^3} + \tilde{f}(\tilde{\eta},p)\frac{\partial^2\tilde{f}(\tilde{\eta},p)}{\partial\tilde{\eta}^2} - \left(\frac{\partial\tilde{f}(\tilde{\eta},p)}{\partial\tilde{\eta}}\right)^2 + \varepsilon^2 \\ +M\left(\frac{\partial\tilde{f}(\tilde{\eta},p)}{\partial\tilde{\eta}} - \epsilon\right)\Big) + \Omega\left(\frac{\partial\tilde{f}(\tilde{\eta},p)}{\partial\tilde{\eta}} - \epsilon\right), \end{matrix} \tag{4.21}$$

$$N_{\tilde{\theta}}\left[\tilde{\theta}(\tilde{\eta},p)\right] = \begin{matrix} \frac{1}{Pr}\left(\frac{\partial^2\tilde{\theta}(\tilde{\eta},p)}{\partial\tilde{\eta}^2}\right) + \tilde{f}(\tilde{\eta},p)\left(\frac{\partial\tilde{\theta}(\tilde{\eta},p)}{\partial\tilde{\eta}}\right) \\ -n\left(\frac{\partial\tilde{f}(\tilde{\eta},p)}{\partial\tilde{\eta}}\right)\tilde{\theta}(\tilde{\eta},p) + \gamma\,\tilde{\theta}\,(\tilde{\eta},\mathrm{p}). \end{matrix} \tag{4.22}$$

where $h_{\tilde{f}}$ and $h_{\tilde{\theta}}$ appear to be auxiliary parameters, p denotes the embedding parameter and range 0 to 1.

4.4.2 m^{th}-Order Deformation

$$L_{\tilde{f}}\left[\tilde{f}_m(\tilde{\eta}) - x\tilde{f}_{m-1}(\tilde{\eta})\right] = h_{\tilde{f}} R_m^{\tilde{f}}(\tilde{\eta}), \tag{4.23}$$

$$L_{\tilde{\theta}}\left[\tilde{\theta}_m(\tilde{\eta}) - x\tilde{\theta}_{m-1}(\tilde{\eta})\right] = h_{\tilde{\theta}} R_m^{\tilde{\theta}}(\tilde{\eta}), \tag{4.24}$$

$$\tilde{f}_m(0) = 0, \quad \tilde{f}_m'(0) = 0, \quad \tilde{f}_m'(\infty) = 0, \tag{4.25}$$

$$\tilde{\theta}_m(0) = 0\,, \quad \tilde{\theta}_m(\infty) = 0. \tag{4.26}$$

Nonlinear operators are defined as:

$$R_m^{\tilde{f}}(\tilde{\eta}) = \begin{matrix} \tilde{f}_{m-1}''' + \sum_{k=0}^{m-1}\left[\tilde{f}_{m-1-k}\tilde{f}_k'' - \tilde{f}_{m-1-k}\tilde{f}_k'\right] + \varepsilon^2(1 - \mathrm{x}_m) \\ +\varepsilon(M - \Omega)(1 - \mathrm{x}_m) - M\tilde{f}_{m-1}' + \Omega\left(\tilde{f}_{m-1}'\right), \end{matrix} \tag{4.27}$$

$$R_m^{\tilde{\theta}}(\tilde{\eta}) = \tilde{\theta}_{m-1}'' + \sum_{k=0}^{m-1}\left[\tilde{f}_{m-1-k}\tilde{\theta}_k'\right] - n\left(\tilde{\theta}_{m-1-k}\tilde{f}_k'\right) + \gamma\,\tilde{\theta}_{m-1}. \tag{4.28}$$

$$x_m = \begin{cases} 0, & m \le 1 \\ 1, & m > 1 \end{cases}$$

At $p = 0$ and $p = 1$:

$$\tilde{f}(\tilde{\eta}, 0) = \tilde{f}_0(\tilde{\eta}), \qquad \tilde{f}(\tilde{\eta}, 1) = \tilde{f}(\tilde{\eta}), \tag{4.29}$$

$$\tilde{\theta}(\tilde{\eta}, 0) = \tilde{\theta}_0(\tilde{\eta}), \qquad \tilde{\theta}(\tilde{\eta}, 1) = \tilde{\theta}(\tilde{\eta}). \tag{4.30}$$

Using Taylor series gives final solution when $p = 1$,we have:

At $p = 1$,

$$\tilde{f}(\tilde{\eta}) = \tilde{f}_0(\tilde{\eta}) + \sum_{m=0}^{\infty}\tilde{f}_m(\tilde{\eta}), \tag{4.31}$$

$$\tilde{\theta}(\tilde{\eta}) = \tilde{\theta}_0(\tilde{\eta}) + \sum_{m=0}^{\infty}\tilde{\theta}_m(\tilde{\eta}). \tag{4.32}$$

The approximate solutions are given as follows:

$$\tilde{f}_m(\tilde{\eta}) = \tilde{f}_m^* + A + Be^{-\tilde{\eta}} + Ce^{-\tilde{\eta}}, \tag{4.33}$$

$$\tilde{\theta}_m(\tilde{\eta}) = \tilde{\theta}_m^* + De^{-\tilde{\eta}} + Ee^{-\tilde{\eta}}. \tag{4.34}$$

where, $\tilde{f}_m(\tilde{\eta})$ and $\tilde{\theta}_m(\tilde{\eta})$ are the special solution

4.5 Convergence of Approximate Solutions

The convergence necessary for the homotopic computation of solutions is shown in Fig. 4.2 by the h-curves. The ranges of the converging regions for the auxiliary parameters $h_{\tilde{f}}$ and $h_{\tilde{\theta}}$ are $-1.5 \le h_{\tilde{f}} \le -0.6$ and $-1.9 \le h_{\tilde{\theta}} \le 0.1$.

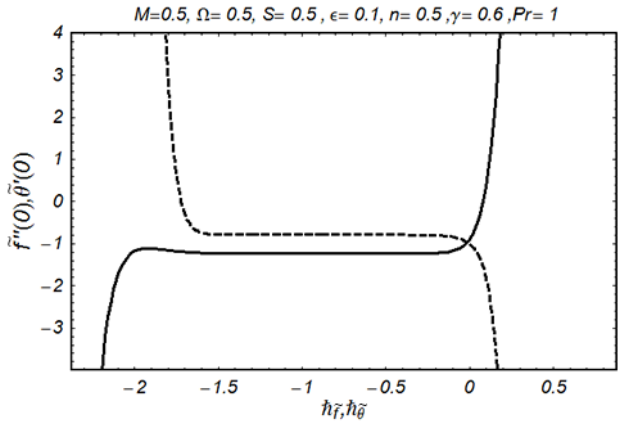

Fig. 4.2: $\tilde{f}''(0)$ and $\tilde{\theta}'(0)$ for h-curves

4.6 Interpretation of Outcomes

This section discusses the properties of the thermal and velocity profiles that correlate to different developing parameters. Fig. 4.3 depicts the ratio of free stream velocity to stretching velocity. Physically, an indicates that free stream velocity is larger than stretching velocity, resulting in increased straining movement fluids closer to the stagnation point at the solid plate, which increases fluid flow rates. According to Fig. 4.4, the velocity profile increases as the magnetic parameter increases. Physically, applying a magnetic field flow creates a drag force known as the Lorentz force to increase magnetic parameters and cause fluid distortion to diminish. The Lorentz force tends to slow down fluid movement at the boundary layer while opposing the transport phenomena. The velocity profile decrease for a greater permeability value was depicted in Fig. 4.5. Fluid motion at the boundary surface is caused by fluid flow through a porous surface. Increased permeability permits a little quantity of fluid to enter through the porous surface of the material. As a result, the velocity of a fluid particle decays. Fig. 4.6 depicts the reduction in velocity field for increasing suction parameter. As the suction parameter rises, the evacuate fluid particle increases, causing resistance behavior between fluid particles. As a result, the velocity of the fluid particle reduces. Fig. 4.7 depicts the rise in velocity field with increasing injection parameter. Increased injection parameters result in increased fluid particle entry into a system. As a result, the flow behavior exhibits an increase in fluid velocity. Fig. 4.8 depicts the behavior of the increase in skin friction with increasing magnetic parameter and

permeability parameter since both parameters demonstrate resistance between fluid particles. Fig. 4.9 illustrates that increasing the P_r number reduces the temperature profile. Since, P_r is the ratio of momentum diffusion to thermal diffusivity, fluid exhibits thermal conduction due to an increase in thermal diffusivity for small P_r numbers. Increases in P_r number slow down temperature transfer from plate surface to fluid particle and reduce boundary layer thickness. Fig. 4.10 demonstrates that increasing the heat source parameter raises the temperature profile. Because the introduction of heat source to the system increases volumetric heat generation. As the temperature of the system rises, so does the temperature field. Fig. 4.11 depicts the temperature profile decreasing when the heat sink parameter is increased. The increased heat absorption coefficient is due to the system receiving the least amount of heat. As a result, the temperature profile decreases.

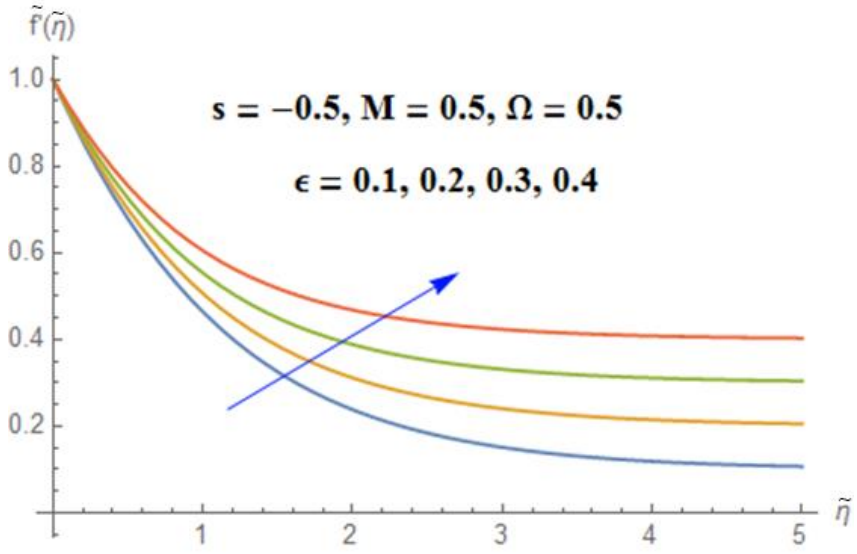

Fig. 4.3: Flow field via ϵ

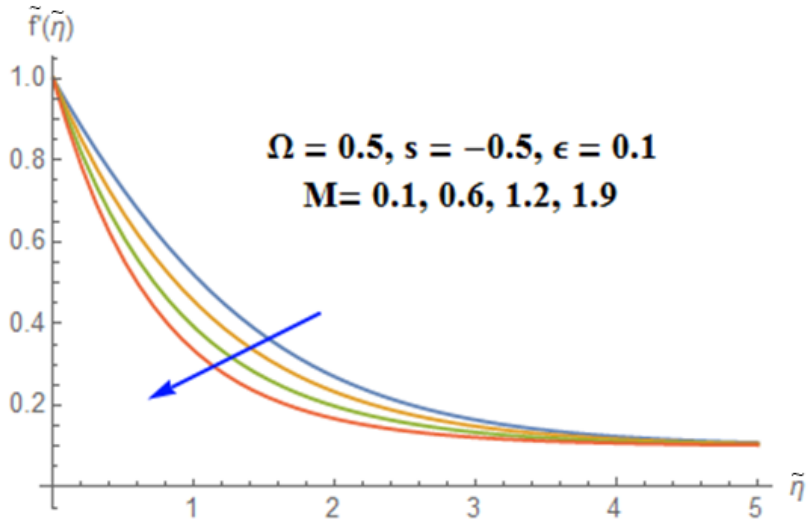

Fig. 4.4: Flow field via *M*

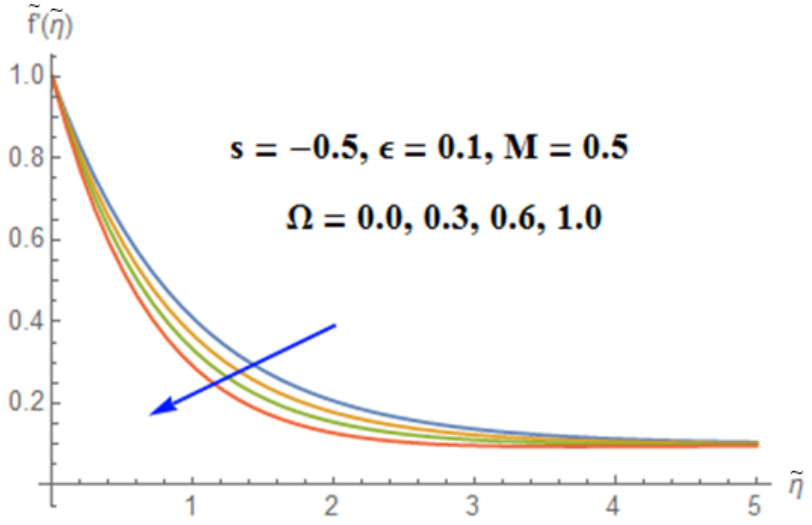

Fig. 4.5: Flow field via Ω

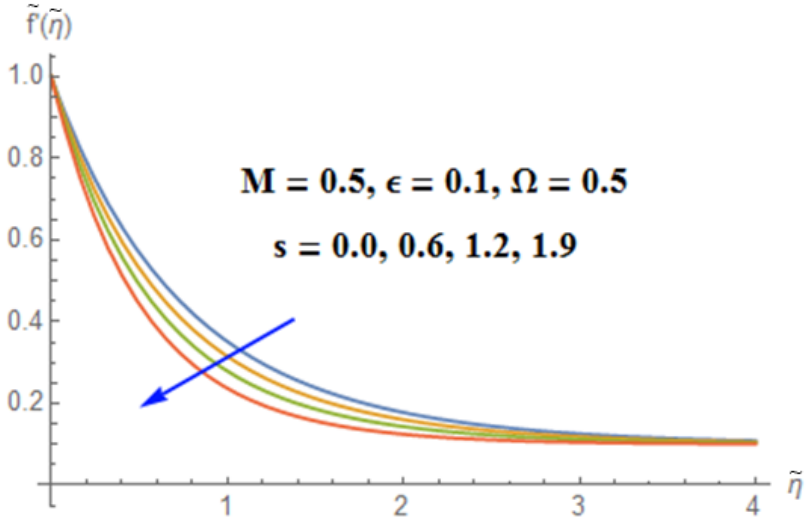

Fig. 4.6: Flow field via $s > 0$

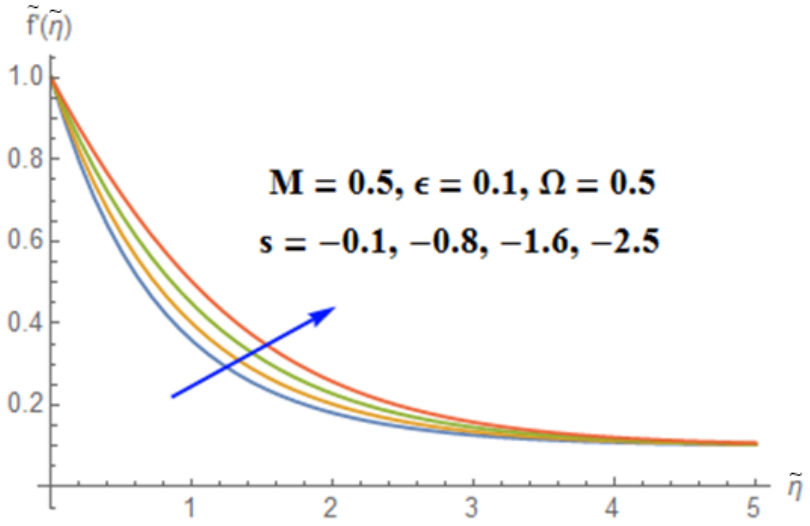

Fig. 4.7: Flowfield via $s < 0$

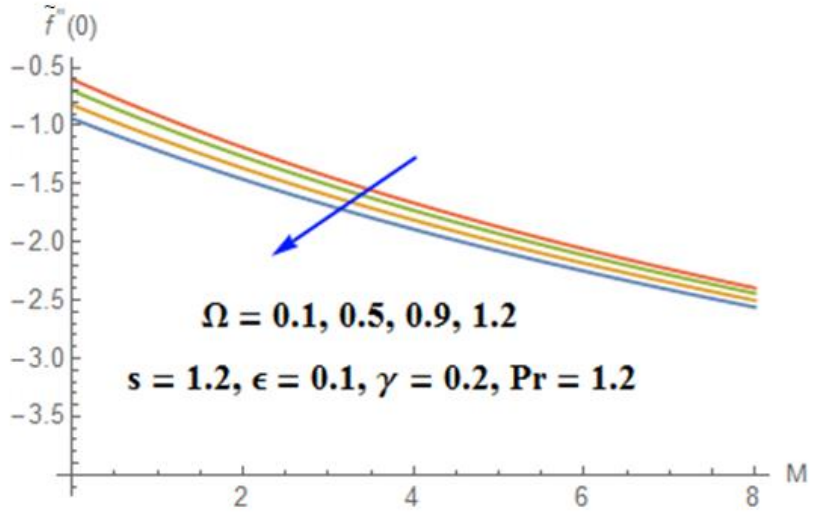

Fig. 4.8: Ω and M via $\tilde{f}''(0)$

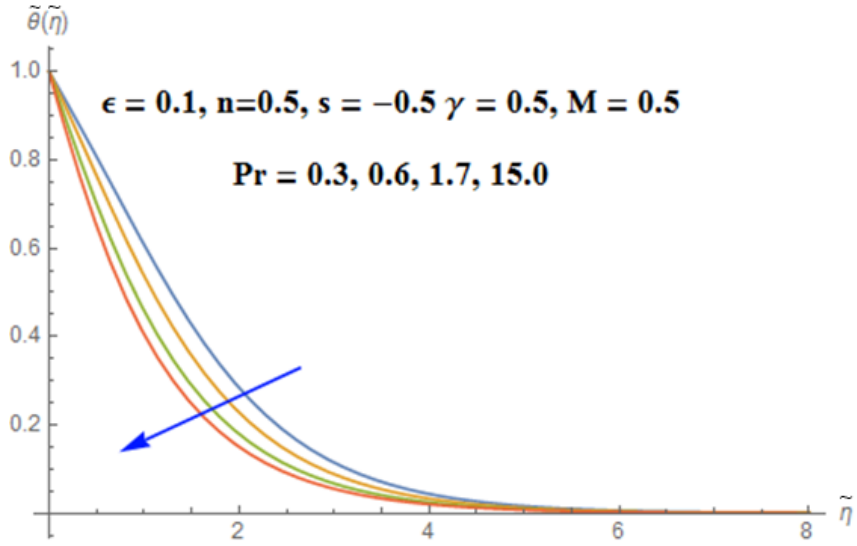

Fig. 4.9: Thermal field via P_r

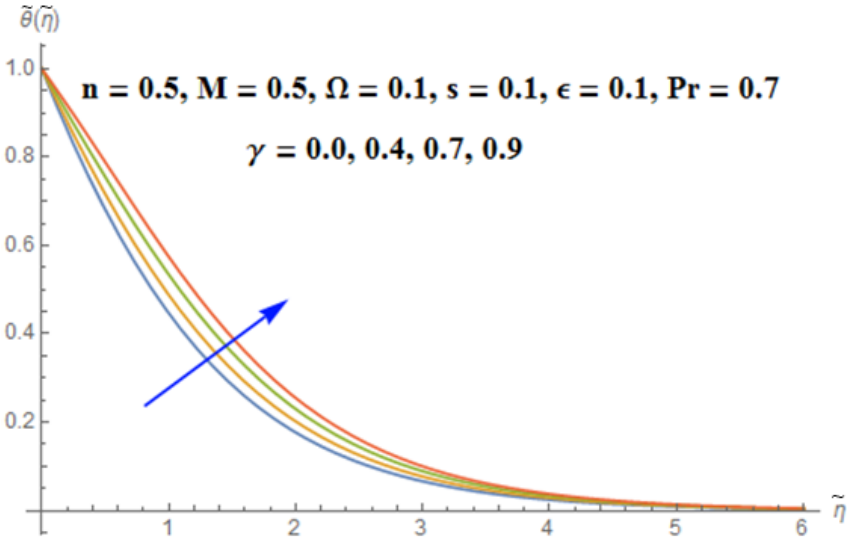

Fig. 4.10: Thermal field via $\gamma > 0$

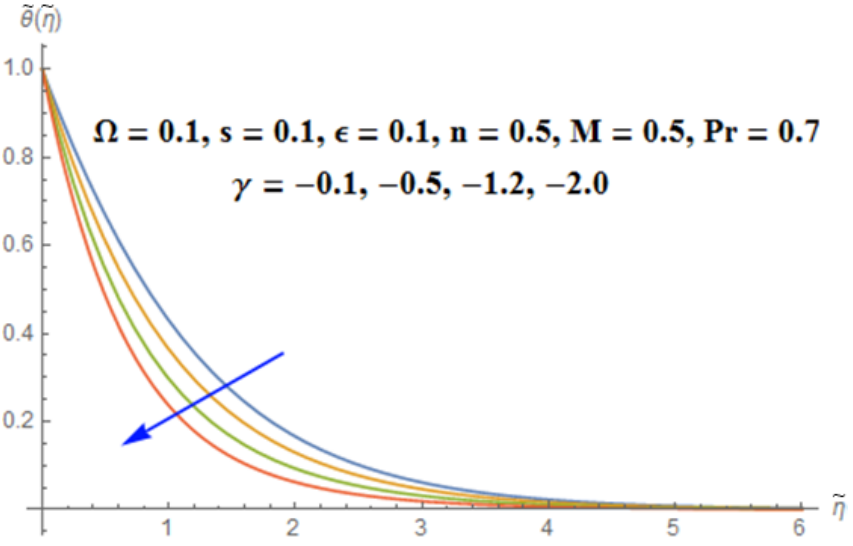

Fig. 4.11: Thermal field via $\gamma < 0$

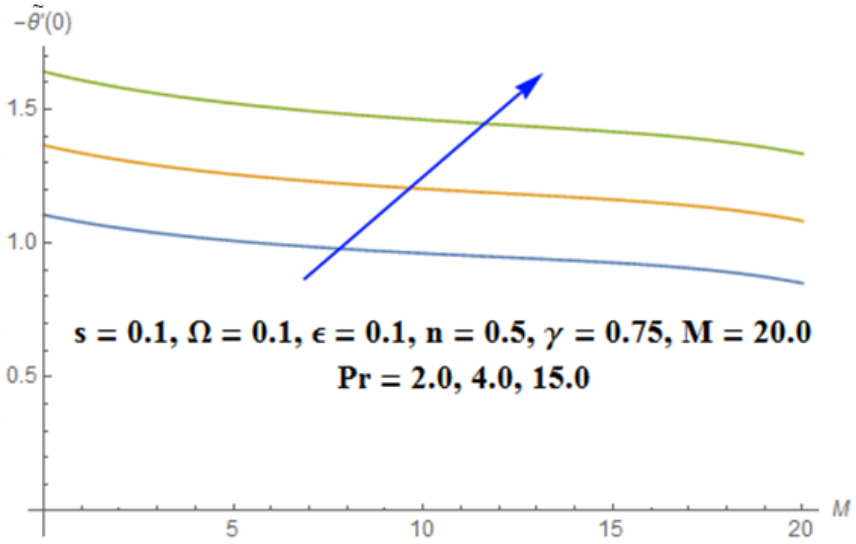

Fig. 4.12: M and P_r via $-\tilde{\theta}'(0)$

CHAPTER 5

FEATURES OF SLIP PHENOMENON IN DOUBLE STRATIFIED FLUID FLOW WITH VISCOUS DISSIPATION AND JOULE HEATING

5.1 Introduction

This section describes the characteristics of a steady, two-dimensional flow of a viscous fluid that had been distorted by a stretched sheet that was placed horizontally. A vertical magnetic field is applied to the fluid flow as it passes through porous material. The fluid flow is also affected by mass and heat transfer, viscous dissipation, linear double stratified flow, and ohmic heating. The permeable wall of plate is also subject to temperature, velocity and concentration slips. The Navier-Stokes equation that emerges are modified using suitable transformations, and analytical convergence solutions are produced using the homotopic methodology. The behavior of the temperature, velocity, and concentration fields are discussed in detail using various parameters, both graphically and physically. The surface heat transfer rate and drag force are also analyzed in relation to certain important parameters. Finally, it is demonstrated that the main stratification phenomena reduce both the solutal and energy profile.

5.2 Problem Statement

This study investigates the magnetization of viscous fluid particles by a stationary, incompressible, and infinitely long horizontal surface displays linear stretching behavior in the x-direction. The free stream velocity is assumed to be $\widetilde{U}_{\infty}(x) = bx$. The strength of magnetic field subjected to the moving fluid inside the normal direction. For the transmission of energy, ohmic heating and viscous dissipation are accounted. Slip processes are also involved in thermal, velocity, and solutal slips across porous media. Temperature and concentration are thought to alter at the plate wall and in the surrounding area. The following continuity, momentum, and concentration equations are obtained using boundary flows theory.

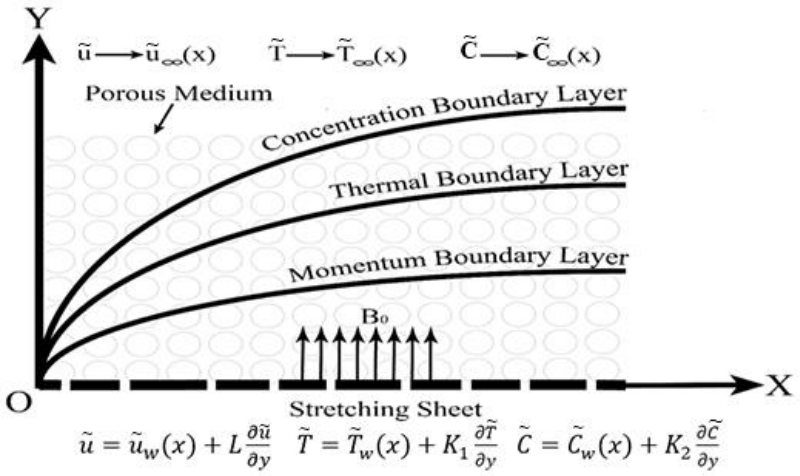

Fig. 5.1: Flow Model

$$\frac{\partial \tilde{u}}{\partial x} + \frac{\partial \tilde{v}}{\partial y} = 0, \tag{5.1}$$

$$\tilde{u}\frac{\partial \tilde{u}}{\partial x} + \tilde{v}\frac{\partial \tilde{v}}{\partial y} = \tilde{U}_\infty \frac{d\tilde{U}_\infty}{dx} + \nu\frac{\partial^2 \tilde{u}}{\partial y^2} + \frac{\sigma {B_0}^2}{\rho}\left(\tilde{U}_\infty - \tilde{u}\right) - \frac{\nu}{K}\left(\tilde{u} - \tilde{U}_\infty\right), \tag{5.2}$$

$$\tilde{u}\frac{\partial \tilde{T}}{\partial x} + \tilde{v}\frac{\partial \tilde{T}}{\partial y} = \alpha\frac{\partial^2 \tilde{T}}{\partial y^2} + \frac{\mu}{\rho C_p}\left(\frac{\partial \tilde{u}}{\partial y}\right)^2 + \frac{\sigma}{\rho C_p}B_o^2\tilde{u}^2, \tag{5.3}$$

$$\tilde{u}\frac{\partial \tilde{C}}{\partial x} + \tilde{v}\frac{\partial \tilde{C}}{\partial y} = D\frac{\partial^2 \tilde{C}}{\partial y^2}. \tag{5.4}$$

The relevant boundary conditions are given as follows:

$$\tilde{u} = \tilde{U}_w(x) + L\frac{\partial \tilde{u}}{\partial y}, \tag{5.5}$$

$$\tilde{T} = \tilde{T}_w(x) + K_1\frac{\partial \tilde{T}}{\partial y}, \tag{5.6}$$

$$\tilde{C} = \tilde{C}_w(x) + K_2\frac{\partial \tilde{C}}{\partial y}. \tag{5.7}$$

$$\tilde{U}_\infty(x) = bx \quad as \quad \tilde{\eta} \to \infty, \tag{5.8}$$

$$\tilde{T}_\infty(x) = \tilde{T}_O + e_2 x \quad as \quad \tilde{\eta} \to \infty, \tag{5.9}$$

$$\tilde{C}_\infty(x) = \tilde{C}_O + d_2 x \quad as \quad \tilde{\eta} \to \infty \tag{5.10}$$

$$\tilde{u} = \tilde{U}_w(x) = ax, \tag{5.11}$$

$$\tilde{T}_w(x) = \tilde{T}_O + e_1 x, \tag{5.12}$$

$$\tilde{C}_w(x) = \tilde{C}_O + d_1 x. \tag{5.13}$$

In this case, the terms $\tilde{u}$ and $\tilde{v}$ reflects the velocity components in two-dimensional flow respectively. viscosity is depicted by μ, specific energy capacity at constant flow rate is denoted by c_p, Momentum diffusivity is denoted by ν, density is symbolized by ρ, B_0 indicates a magnetic field, thermal diffusivity reflects α, permeability of porous material is represented by K and σ stands for the electrical conductivity, $\tilde{C}_w$ and $\tilde{T}_w$ indicates concentration and temperature adjacent to the wall, D indicates molecular diffusion rate, $\tilde{C}_\infty$and $\tilde{T}_\infty$ depict ambient concentration and temperature respectively, and $\widetilde{U}_w$ for wall velocity at wall, $\widetilde{U}_\infty$ indicates ambient velocity.

5.3 Transformations

The transformations for the current governing flow problem are as follows:

$$\tilde{f}'(\tilde{\eta}) = \frac{\psi}{(av)^{\frac{1}{2}}x}, \tilde{\theta}(\tilde{\eta}) = \frac{(\tilde{T}-\tilde{T}_\infty)}{(\tilde{T}_w-\tilde{T}_0)}, \quad \tilde{\phi}(\tilde{\eta}) = \frac{(\tilde{C}-\tilde{C}_\infty)}{(\tilde{C}_w-\tilde{C}_0)}, \tilde{\eta} = (\tfrac{a}{\nu})^{\frac{1}{2}} y. \tag{5.14}$$

The following are the coefficient of velocity vector:

$$\tilde{u} = \tilde{f}'(\tilde{\eta}), \tilde{v} = (av)^{\frac{1}{2}}\widetilde{f}\,(\tilde{\eta}). \tag{5.15}$$

Non-dimensional ordinary differential equations based on the abovementioned transformations are as follows:

$$\tilde{f}''' + \tilde{f}\tilde{f}'' - \tilde{f}'^2 + M\left(\epsilon - \tilde{f}'\right) - \Omega\left(\epsilon - \tilde{f}'\right) = 0, \tag{5.16}$$

$$\frac{1}{Pr}\tilde{\theta}'' + \tilde{f}\tilde{\theta}' - \tilde{f}'\tilde{\theta} - \epsilon_1\tilde{f}' + E_c\tilde{f}''^2 + ME_c\tilde{f}'^2 = 0, \tag{5.17}$$

$$\frac{1}{S_C}\tilde{\phi}'' + \tilde{f}\tilde{\phi}' - \tilde{f}'\tilde{\phi} - \epsilon_2\tilde{f}' = 0. \tag{5.18}$$

The relevant boundary conditions are:

$$\tilde{\mathrm{f}}'(0) = 1 + S_1\tilde{\mathrm{f}}''(0), \qquad \tilde{\mathrm{f}}(0) = 0, \qquad \tilde{\mathrm{f}}'(\infty) = \epsilon, \tag{5.19}$$

$$\tilde{\theta}(0) = 1 - \epsilon_1 + \mathrm{S}_2\tilde{\theta}'(0), \qquad \tilde{\theta}(\infty) = 0, \tag{5.20}$$

$$\widetilde{\phi}(0) = 1 - \epsilon_2 + \mathrm{S}_3\widetilde{\phi}'(0), \qquad \widetilde{\phi}(\infty) = 0. \tag{5.21}$$

Now, Prandtl number is displayed by P_r, $\epsilon_2$depicts solutal stratified parameter, s_2 reflects thermal slip, Ω denotes permeability of porous medium, ε_1 shows thermal stratified parameter,

Sc denotes the Schmidt number, ϵ depicts velocity ratio parameter, Ec indicates the Eckert number, s_1 denotes velocity slip, M stand for magnetic field parameter and s_3 reveals solutal slip, as below

$$P_r = \frac{\nu}{\alpha}, \qquad \varepsilon_2 = \frac{d_1}{d_2}, \qquad s_2 = k_1\left(\frac{a}{\nu}\right)^{\frac{1}{2}},$$

$$\Omega = \frac{\nu}{ak}, \qquad \varepsilon_1 = \frac{e_1}{e_2}, \qquad E_c = \frac{a^2 x}{e_1 c_p} \quad ,$$

$$s_1 = L\left(\frac{a}{\nu}\right)^{\frac{1}{2}}, \quad M = \frac{\sigma {B_0}^2}{a\rho}, \quad s_3 = k_2\left(\frac{a}{\nu}\right)^{\frac{1}{2}}.$$

5.4 Homotopic Solutions

The following are approximation:

$$\widetilde{f_0}(\tilde{\eta}) = \varepsilon\tilde{\eta} + \frac{(1-\epsilon)-(1-e^{-\tilde{\eta}})}{1+S_1}, \tag{5.22}$$

$$\tilde{\theta}_0(\tilde{\eta}) = \frac{(1-\epsilon_1)e^{-\tilde{\eta}}}{1+S_2}, \tag{5.23}$$

$$\tilde{\phi}_0(\tilde{\eta}) = \frac{(1-\epsilon_2)e^{-\tilde{\eta}}}{1+S_3}. \tag{5.24}$$

The variable $\tilde{f}$, $\tilde{\theta}$ and $\tilde{\phi}$ have the linear operators shown below:

$$L_{\tilde{f}} = \frac{d^3\tilde{f}}{d\tilde{\eta}^3} - \frac{d\tilde{f}}{d\tilde{\eta}}, \tag{5.25}$$

$$L_{\tilde{\theta}} = \frac{d^2\tilde{\theta}}{d\tilde{\eta}^2} - \tilde{\theta}, \tag{5.26}$$

$$L_{\tilde{\phi}} = \frac{d^2\tilde{\phi}}{d\tilde{\eta}^2} - \tilde{\phi}. \tag{5.27}$$

It can be seen how the following equation is satisfied,

$$L_{\tilde{f}}\left(A + Be^{-\tilde{\eta}} + Ce^{-\tilde{\eta}}\right), \tag{5.28}$$

$$L_{\tilde{\theta}}\left(De^{-\tilde{\eta}} + Ee^{-\tilde{\eta}}\right), \tag{5.29}$$

$$L_{\tilde{\phi}}(Fe^{-\tilde{\eta}} + Ge^{-\tilde{\eta}}). \tag{5.30}$$

Arbitrary constants are displayed from $A\ to\ G$.

5.4.1 Zeroth-Order Deformation

The following zeroth order governing equation are as follows:

$$(1-p)L_{\tilde{f}}\left[\tilde{f}(\tilde{\eta},p)-\tilde{f}_0(\tilde{\eta})\right]=ph_{\tilde{f}}N_{\tilde{f}}[\tilde{f}(\tilde{\eta},p)], \tag{5.31}$$

$$(1-p)L_{\tilde{\theta}}\left[\tilde{\theta}(\tilde{\eta},p)-\tilde{\theta}_0(\tilde{\eta})\right]=ph_{\tilde{\theta}}N_{\tilde{\theta}}[\tilde{f}(\tilde{\eta},p),\tilde{\theta}(\tilde{\eta},p)], \tag{5.32}$$

$$(1-p)L_{\tilde{\phi}}\left[\tilde{\phi}(\tilde{\eta},p)-\tilde{\phi}_0(\tilde{\eta})\right]=ph_{\tilde{\phi}}N_{\tilde{\phi}}[\tilde{f}(\tilde{\eta},p),\tilde{\theta}(\tilde{\eta},p),\tilde{\phi}(\tilde{\eta},p)]. \tag{5.33}$$

with the below mentioned border conditions:

$$\tilde{f}(0,p)=0,\quad \tilde{f}'(0,p)=1+s_1\tilde{f}''(0,p),\quad \tilde{f}'(\infty,p)\to\varepsilon, \tag{5.34}$$

$$\tilde{\theta}(0,p)=1-\epsilon_1+s_2\tilde{\theta}'(0,p),\qquad \tilde{\theta}(\infty,p)\to 0. \tag{5.35}$$

$$\tilde{\phi}(0,p)=1-\epsilon_1+s_2\tilde{\phi}'(0,p),\qquad \tilde{\phi}(\infty,p)\to 0. \tag{5.36}$$

Here, the embedded variable $N_{\tilde{f}}$ and $N_{\tilde{\theta}}$ are non-linear operators are provided as follows:

$$N_{\tilde{f}}\left[\tilde{f}(\tilde{\eta},p)\right]=\begin{matrix}\frac{\partial^3\tilde{f}(\tilde{\eta},p)}{\partial\tilde{\eta}^3}+\tilde{f}(\tilde{\eta},p)\frac{\partial^2\tilde{f}(\tilde{\eta},p)}{\partial\tilde{\eta}^2}-\left(\frac{\partial\tilde{f}(\tilde{\eta},p)}{\partial\tilde{\eta}}\right)^2\\ +\varepsilon^2+(M+\Omega)\left(\epsilon-\frac{\partial\tilde{f}(\tilde{\eta},p)}{\partial\tilde{\eta}}\right),\end{matrix} \tag{5.37}$$

$$N_{\tilde{\theta}}\left[\tilde{\theta}(\tilde{\eta},p)\right]=\begin{matrix}\frac{1}{Pr}\left(\frac{\partial^2\tilde{\theta}(\tilde{\eta},p)}{\partial\tilde{\eta}^2}\right)+\tilde{f}(\tilde{\eta},p)\left(\frac{\partial\tilde{\theta}(\tilde{\eta},p)}{\partial\tilde{\eta}}\right)-\left(\frac{\partial\tilde{f}(\tilde{\eta},p)}{\partial\tilde{\eta}}\right)\tilde{\theta}(\tilde{\eta},p)\\ +Ec\left(\frac{\partial^2\tilde{f}(\tilde{\eta},p)}{\partial\tilde{\eta}^2}\right)^2+Ec.M\left(\frac{\partial\tilde{f}(\tilde{\eta},p)}{\partial\tilde{\eta}}\right),^2\end{matrix} \tag{5.38}$$

$$N_{\tilde{\phi}}\left[\tilde{\phi}(\tilde{\eta},p)\right]=\begin{matrix}\frac{1}{Sc}\left(\frac{\partial^2\tilde{\phi}(\tilde{\eta},p)}{\partial\tilde{\eta}^2}\right)+\tilde{f}(\tilde{\eta},p)\left(\frac{\partial\tilde{\phi}(\tilde{\eta},p)}{\partial\tilde{\eta}}\right)\\ -\left(\frac{\partial\tilde{f}(\tilde{\eta},p)}{\partial\tilde{\eta}}\right)\tilde{\phi}(\tilde{\eta},p)+\epsilon_2\left(\frac{\partial\tilde{f}(\tilde{\eta},p)}{\partial\tilde{\eta}}\right).\end{matrix} \tag{5.39}$$

$$L_{\tilde{f}}\left[\,\tilde{f}_m(\tilde{\eta})-x_m\tilde{f}_{m-1}(\tilde{\eta})\,\right]=h_{\tilde{f}}R_m^{\tilde{f}}(\tilde{\eta}), \tag{5.40}$$

$$L_{\tilde{\theta}}\left[\,\tilde{\theta}_m(\tilde{\eta})-x_m\tilde{\theta}_{m-1}(\tilde{\eta})\,\right]=h_{\tilde{\theta}}R_m^{\tilde{\theta}}(\tilde{\eta}), \tag{5.41}$$

$$L_{\tilde{\phi}}\left[\,\tilde{\phi}_m(\tilde{\eta})-x_m\tilde{\phi}_{m-1}(\tilde{\eta})\,\right]=h_{\tilde{\phi}}R_m^{\tilde{\phi}}(\tilde{\eta}). \tag{5.42}$$

$$\tilde{f}_m(0)=0,\quad \tilde{f}_m'(0)=0,\quad \tilde{f}_m'(\infty)=0, \tag{5.43}$$

$$\tilde{\theta}_m(0)=s_2\tilde{\theta}_m(0),\qquad \tilde{\theta}_m(\infty)=0, \tag{5.44}$$

$$\tilde{\phi}_m(0)=s_3\tilde{\phi}_m(0),\quad \tilde{\theta}_m(\infty)=0. \tag{5.45}$$

Nonlinear operators are defined as:

$$R_m^{\tilde{f}}(\tilde{\eta})=\begin{matrix}\tilde{f}_{m-1}'''+\sum_{k=0}^{m-1}\left[\tilde{f}_{m-1-k}\tilde{f}_k''-\tilde{f}_k'\right]+\varepsilon^2(1-\mathrm{x}_m)\\ +\varepsilon(M-\Omega)(1-\mathrm{x}_m)-M\tilde{f}_{m-1}'-\ \Omega\left(\tilde{f}_{m-1}'\right),\end{matrix} \tag{5.46}$$

$$R_m^{\tilde{\theta}}(\tilde{\eta})=\begin{matrix}\tilde{\theta}_{m-1}''+\sum_{k=0}^{m-1}\left[\tilde{f}_{m-1-k}\tilde{\theta}_k'-\left(\tilde{\theta}_{m-1-k}\tilde{f}_k'\right)\right]\\ +\mathrm{Ec}\left(\tilde{f}_{m-1-k}\tilde{f}_k''\right)+\mathrm{MEc}\left(\tilde{f}'_{m-1-k}\tilde{f}_k'\right),\end{matrix} \tag{5.47}$$

$$R_m^{\tilde{\phi}}(\tilde{\eta})=\tilde{\phi}_{m-1}''+\sum_{k=0}^{m-1}\left[\tilde{f}_{m-1-k}\tilde{\phi}_k'\right]-n\left(\tilde{\phi}_{m-1-k}\tilde{f}_k'\right)+\ \epsilon_2\tilde{f}_k'. \tag{5.48}$$

$$x_m = \begin{cases} 0, & m \leq 1 \\ 1, & m > 1 \end{cases}.$$

The Taylor series as a guide to ultimate approximated result. At $p = 1$, the results are:

$$\tilde{f}(\tilde{\eta}, 0) = \tilde{f}_0(\tilde{\eta}), \qquad \tilde{f}(\tilde{\eta}, 1) = \tilde{f}(\tilde{\eta}). \tag{5.49}$$

$$\tilde{\theta}(\tilde{\eta}, 0) = \tilde{\theta}_0(\tilde{\eta}), \qquad \tilde{\theta}(\tilde{\eta}, 1) = \tilde{\theta}(\tilde{\eta}). \tag{5.50}$$

$$\tilde{\phi}(\tilde{\eta}, 0) = \tilde{\phi}_0(\tilde{\eta}), \qquad \tilde{\phi}(\tilde{\eta}, 1) = \tilde{\phi}(\tilde{\eta}). \tag{5.51}$$

Approximate solution as follows:

$$\tilde{f}_m(\tilde{\eta}) = \tilde{f}_m^* + A + Be^{-\tilde{\eta}} + Ce^{-\tilde{\eta}}, \tag{5.52}$$

$$\tilde{\theta}_m(\tilde{\eta}) = \tilde{\theta}_m^* + De^{-\tilde{\eta}} + Ee^{-\tilde{\eta}}, \tag{5.53}$$

$$\tilde{\phi}_m(\tilde{\eta}) = \tilde{\phi}_m^* + Fe^{-\tilde{\eta}} + Ge^{-\tilde{\eta}}. \tag{5.54}$$

where the solution displayed as $\tilde{f}_m^*, \tilde{\theta}_m^*$ and $\tilde{\phi}_m^*$.

5.5 Convergence Analysis

In order to examine and conform the convergence of approximate results, h-curves are visually produced (see Fig. 5.2). The determined range from of the auxiliary variables for the converging area, $h_{\tilde{f}}$, $h_{\tilde{\theta}}$ and $h_{\tilde{\phi}}$ are from $-1.9 \leq h_{\tilde{f}} \leq -0.2$, -1.8 $h_{\tilde{\theta}}$ -0.2, -2.6 $h_{\tilde{\phi}}$ -0.2.

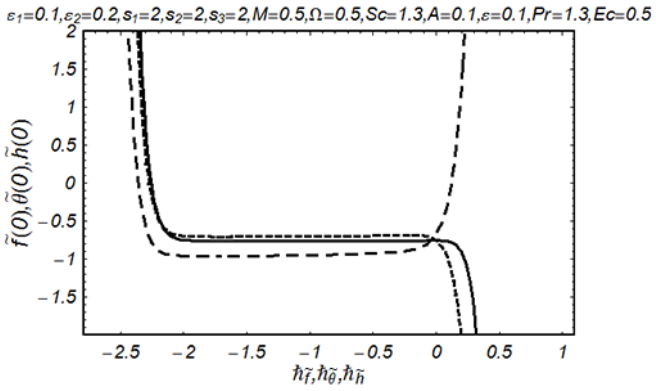

Fig. 5.2: $\tilde{f}''(0)$, $\tilde{\theta}'(0)$ and $\tilde{\phi}'(0)$ via *h*-curves

5.6 Interpretation of Outcomes

The major goal of this part is to visually and physically demonstrate the thermal, velocity, solutal profile that correlate to newly developing parameters. Fig. 5.3 depicts an increase in velocity profile for a greater ratio of velocity parameter due to an increase in free stream velocity parameter, which causes an increase in fluid particle velocity. The effect of magnetic parameters on velocity and temperature fields is depicted in Fig. 5.4 and Fig. 5.5. Because a rise in magnetic parameters results in a drop in fluid particle velocity as well as an increase in Lorentz force, which increases resistance between fluid particles and creates heat. As a result, the temperature of the fluid rises. Fig. 5.6 depicts the increase in velocity field when the permeability parameter is increased. Because a higher permeability value allows for a greater quantity of fluid flow, the velocity of fluid particles increases. Fig. 5.7 depicts the influence of the velocity slip on the velocity distribution. When the slip parameter is increased, the deformation between fluid particles and the stretching sheet decreases. Higher slip indicates more fluid behavior towards the sheet wall as well as increased fluid particles slippages a result, the analysis of the velocity field decreases in the temperature distribution is shown in Fig.5.8 in accordance with the Prandtl number decrement that occurs in the temperature distribution for increasing values of the Prandtl number. The rate of heat transmission from the heated sheet to the fluid is reduced owing to heat transfer degradation caused by dominating Prandtl numbers. Fig. 5.9 depicted the effect of Ec on the temperature field. The system's temperature rises as a result of Increases in Ec number cause heat to be produced when fluid resistance increases. As a result, the temperature profile increases. The temperature profile rises with increasing thermal slip, as seen in Fig.5.10. Because increasing the thermal slip parameter decreases heat transmission from the sheet to the neighboring fluid particles. As a result, the temperature of the fluids drops. Fig. 5.11 depicted the effect of thermal stratification parameters on temperature fields. The increase in thermally stratified parameters divides the molecule of fluid into different sections based on density, which operate as a barrier for heat transit while also increasing the ambient temperature of fluids but decreasing the temperature of the sheet. As a result, the temperature profile falls. The impact of the Schmidt number via concentration differential is seen in Fig. 5.12. The Schmidt number enhances fluid mass diffusion while lowering boundary layer thickness as its value goes up. Fig. 5.13 demonstrates that when the solutal slip parameter increases, the concentration field

decreases due to a decrease in mass diffusion from the plate's surface to the fluids. Fig. 5.14 depicts the drop in concentration fields when the solutal stratified parameter is increased. Increasing the value of the solutal stratification parameter created varied regions of density, which also generated resistance during mass diffusion. Fig. 5.15 depicts the impact of skin friction along the parameters s_1 and M. In terms of physical behavior, skin friction increases with velocity slip and magnetic parameter. Fig. 5.16 depicts the decreasing behavior of the Nusselt number with increasing values of thermal slip s_2 and thermal stratification ϵ_1. Fig. 5.17 indicates an increase in the concentration profile for Schmidt number but a decrease for solutal slip s_3.

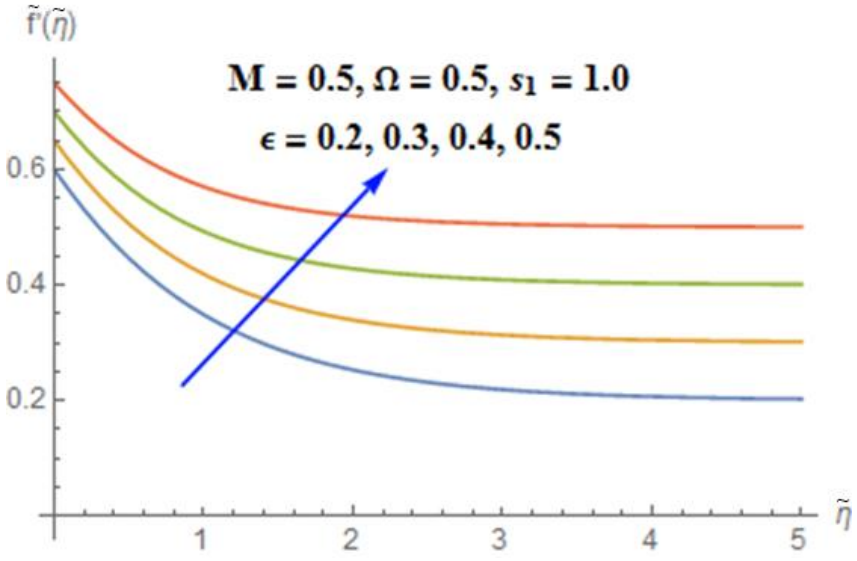

Fig. 5.3: Flow field via ϵ

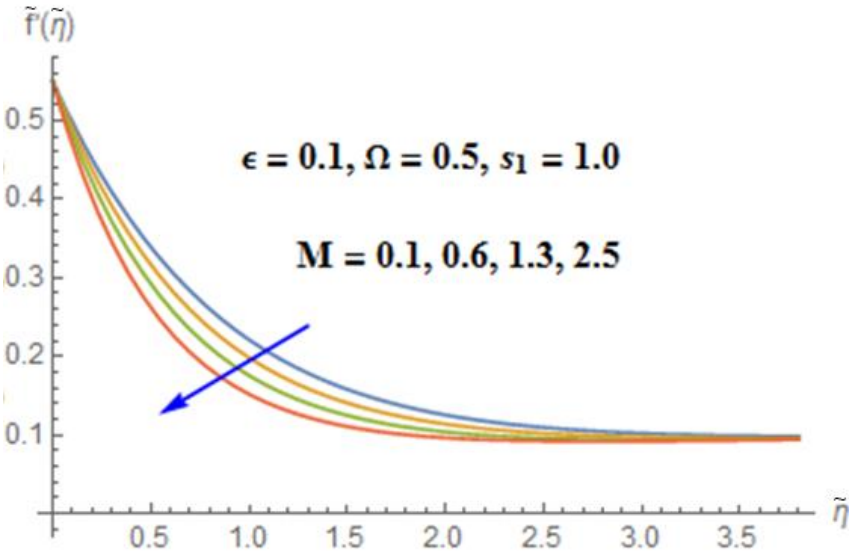

Fig. 5.4: Flow field via *M*

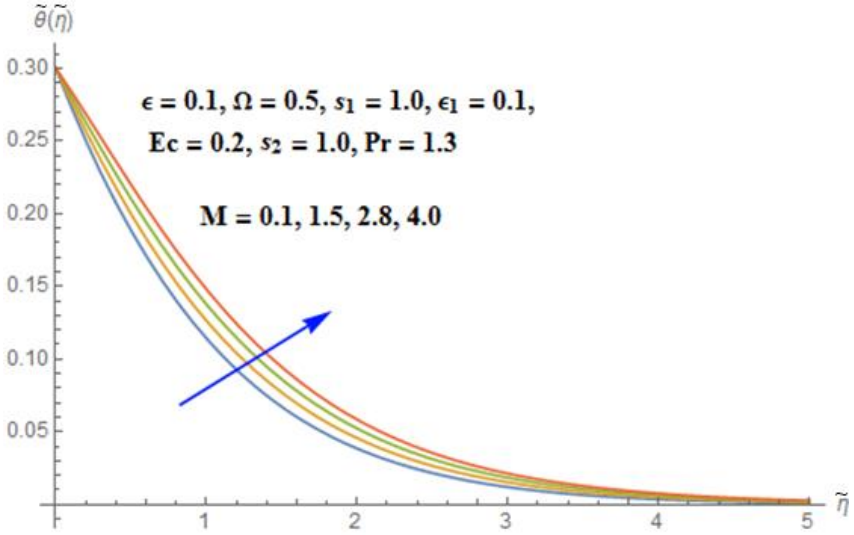

Fig. 5.5: Thermal field via *M*

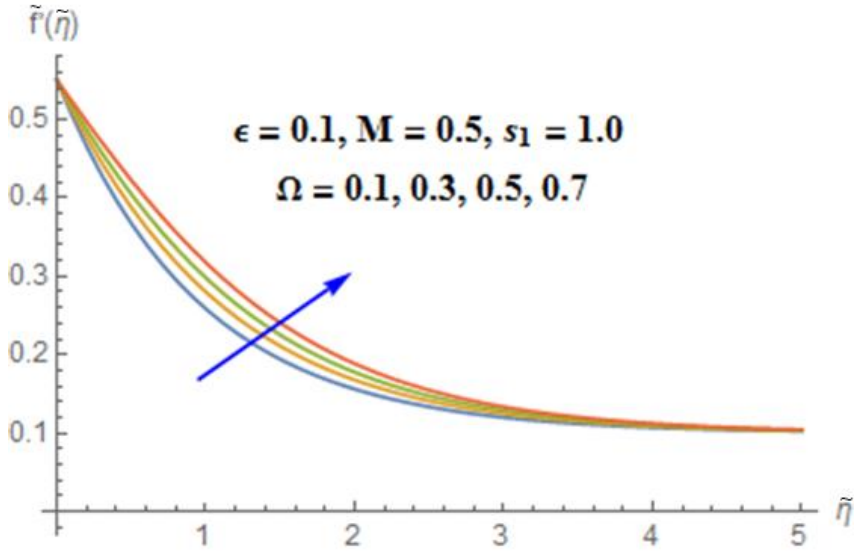

Fig. 5.6: Flow field via Ω

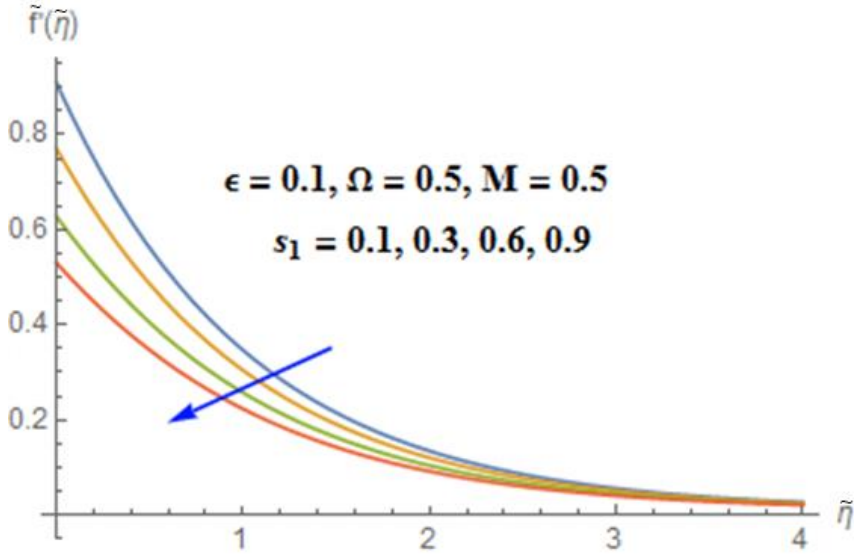

Fig. 5.7: Flow field via s_1

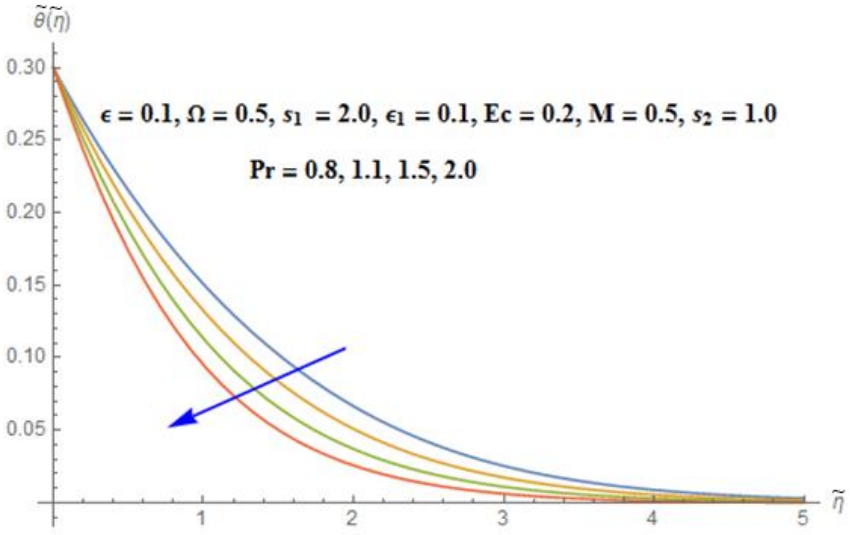

Fig. 5.8: Thermal field via P_r

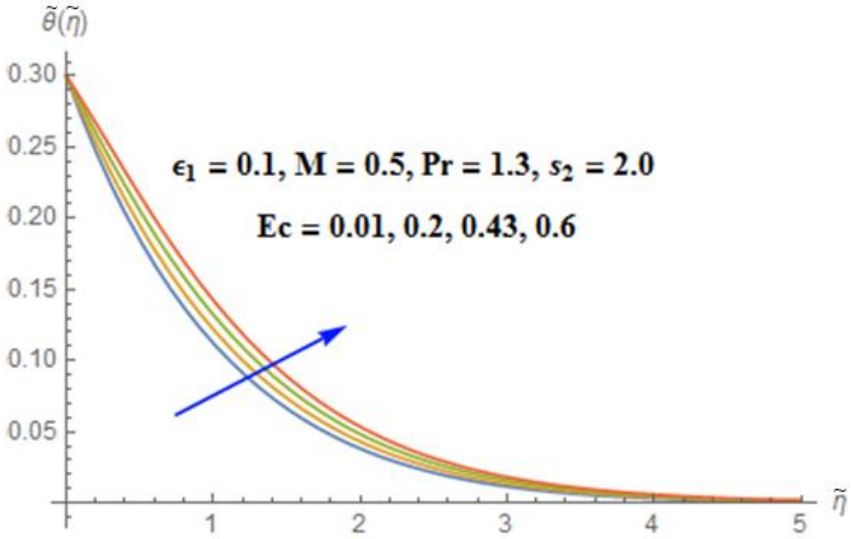

Fig. 5.9: Thermal field via Ec

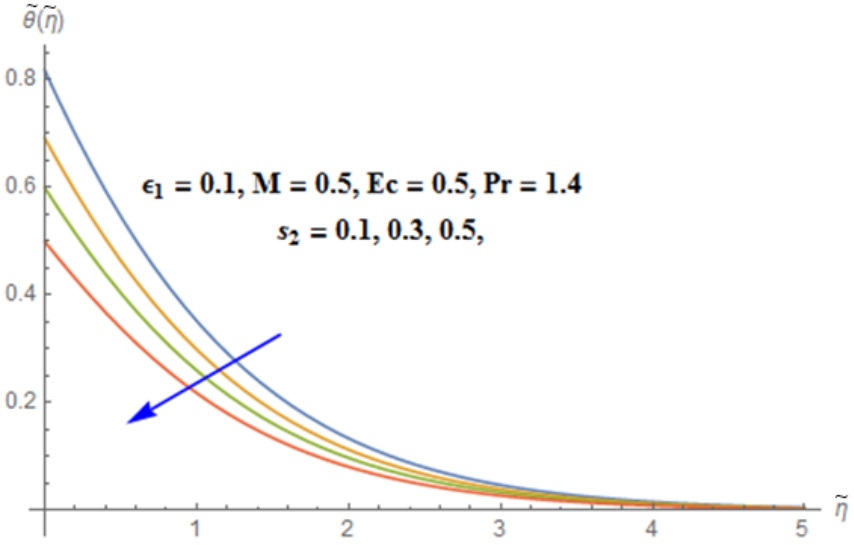

Fig. 5.10: Thermal field via s_2

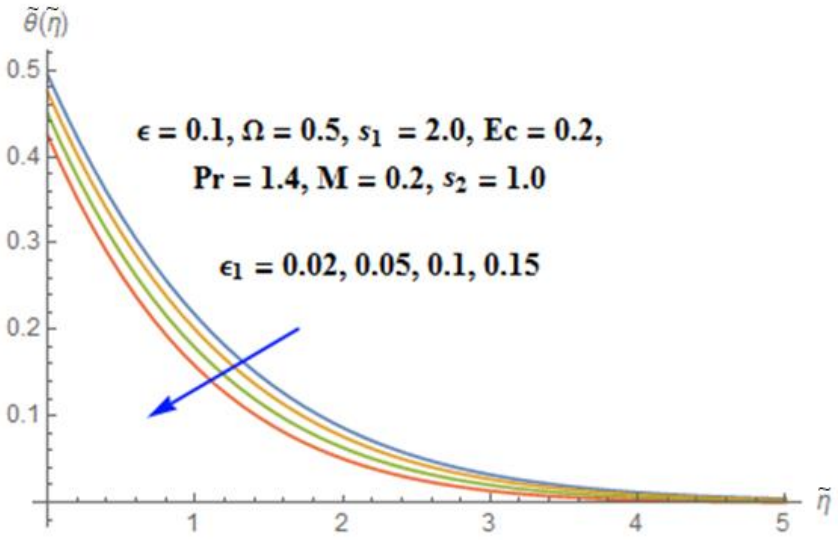

Fig. 5.11: Thermal field via ϵ_1

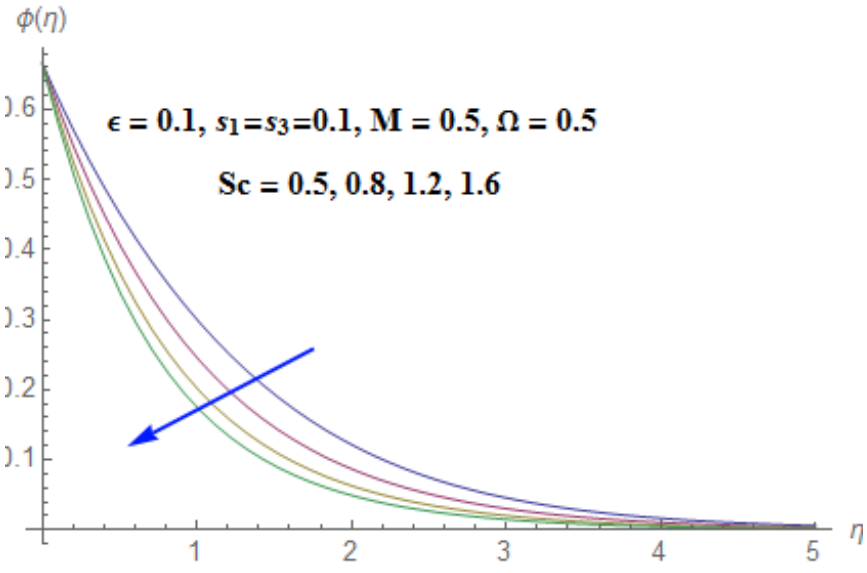

Fig. 5.12: Solutal field via Sc

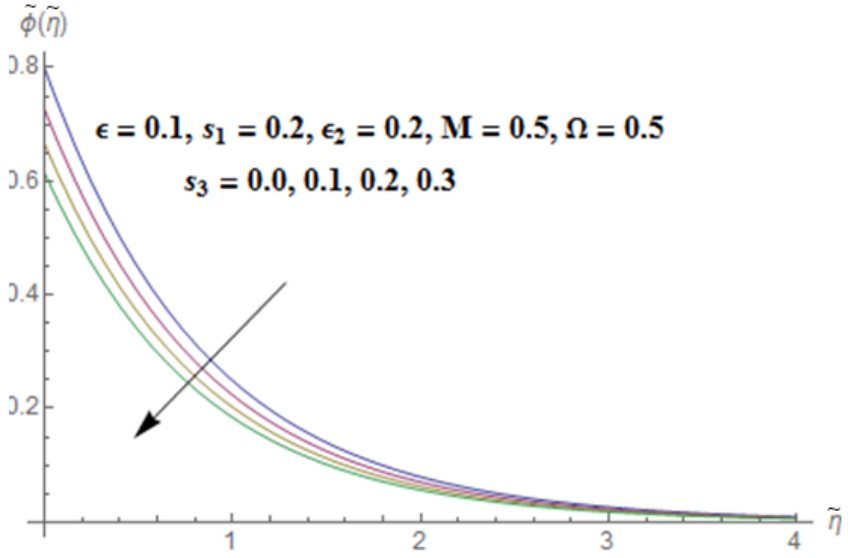

Fig. 5.13: Solutal field via s_3

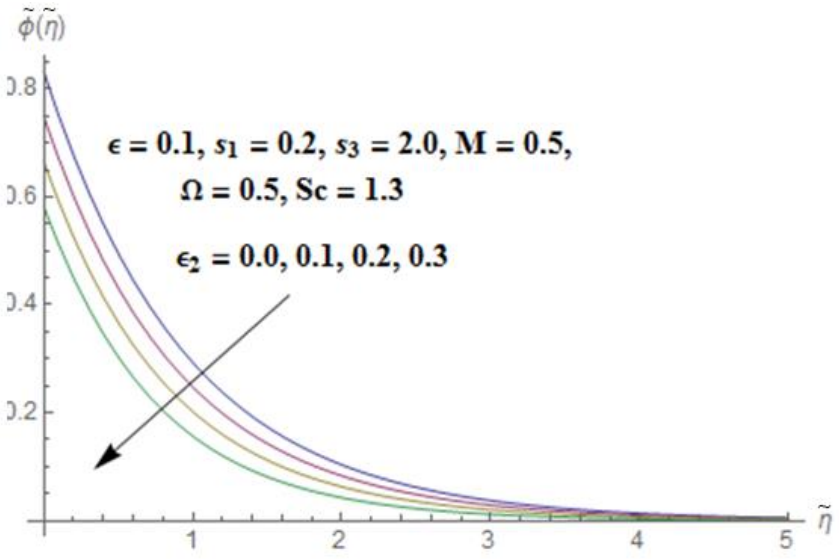

Fig. 5.14: Solutal field via ϵ_2

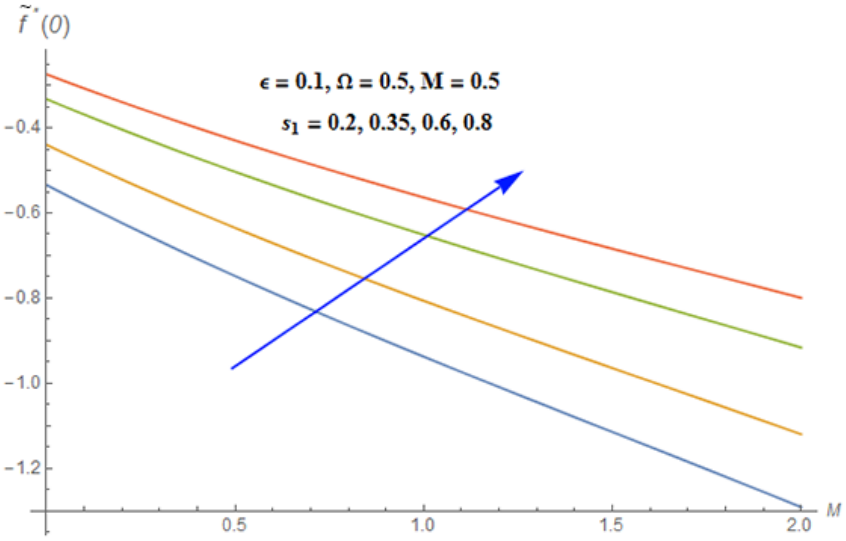

Fig. 5.15: Impact of M and s_1 on $\tilde{f}''(0)$

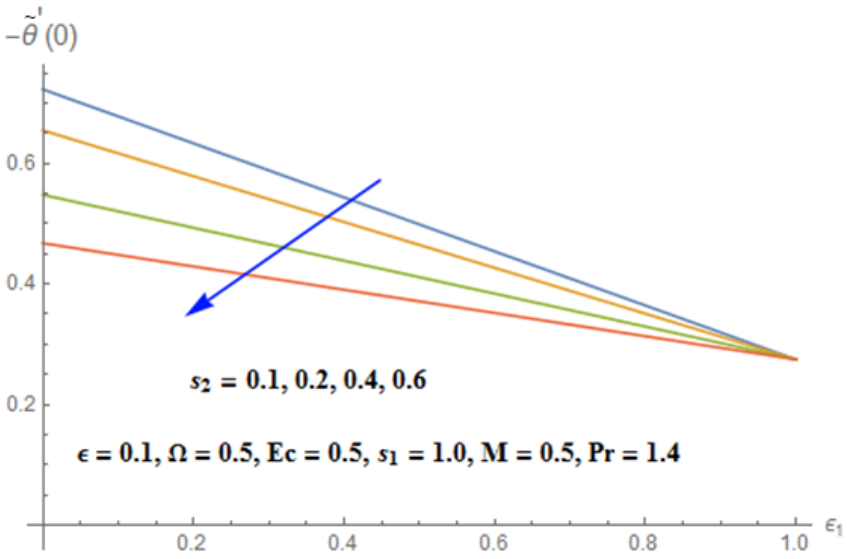

Fig. 5.16: Impact of ϵ_1 and s_2 on $\tilde{\theta}'(0)$

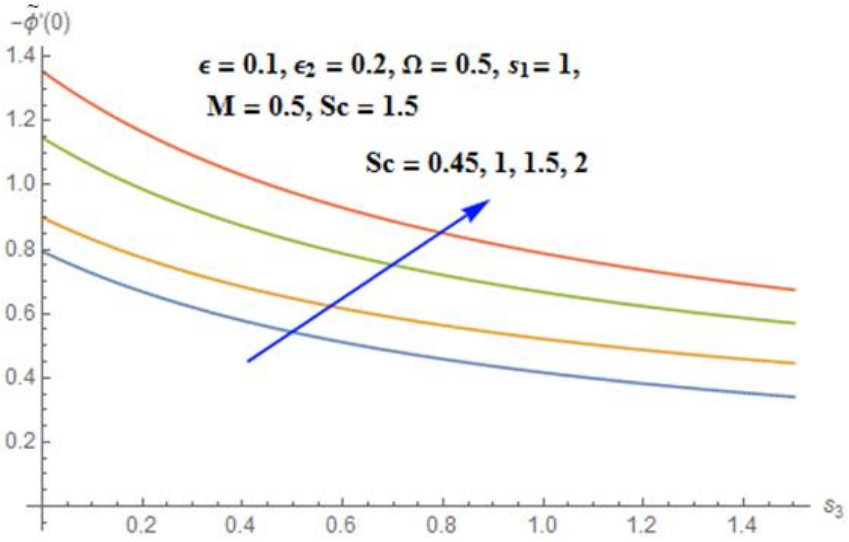

Fig. 5.17: Impact of Sc and s_3 on $\tilde{\phi}'(0)$

CHAPTER 6

CONCLUSION AND FUTURE WORK

6.1 Concluding Remarks

The attempt examines the characteristics of the slip phenomena in viscous flowing fluid, including viscous dissipation, double stratified fluid flow and joule heating. The results found that a strong magnetic component produces a lower velocity profile. The velocity profile is enhanced by growing permeability parameter. The velocity profile is reduced by increasing velocity slip parameter. The temperature field shrinks for dominant thermally stratified factor. The temperature profile decreases when the thermal slip parameter is dominant. The Eckert number is increasing together with the expansion of the temperature distribution. A strong magnetic component produces a higher temperature profile. The solutal profile decreases when the concentration slip parameter is dominant. The solutal stratification parameter decreases the solutal profile. Velocity slip and magnetic parameter increase the coefficient of skin friction. The Nusselt number is reduced under high thermal slip and thermal stratification factors. The Sherwood number against the solutal slip parameter is decreased, and increased by increasing Schmidt number.

The double stratification physical problem has several applications in geophysics, industry, and engineering. The current study is significant since it informs us about the viscous fluid's behavior as it travels through a stretchy sheet when subjected to magnetic forces. The current study can be applied in the chemical processes, bioengineering, thermal treatment of polymers, magnetic processing devices, MHD chromatography technology, fabrication of mono-magnetic material, and manufacturing of micro-roller, hot rolling, productions of glass fiber and paper, twine drawing, spinning of metals, polymer extrusion, and many others.

6.2 Future Work

The present model can prolong for non-Newtonian fluids. The rheological feature of nonlinear fluids can be investigated in presence of Joule heating, in order to explore the properties of fluid will be charged. The present numerical scheme can also be improved for

better of the problem. Nonlinear mixed convection phenomenon can also be studied with the present Stratification process problem for viscous fluid. Stagnation process can also be investigated in micropolar and hybrid nanofluid.

References

[1] Merkin, J. H. and Kumaran, V., (2010). The unsteady MHD boundary-layer flow on a shrinking sheet. European Journal of Mechanics-B/Fluids, 29(5), 357-363.

[2] Escott, L. J. and Griffiths, P. T., (2023). Revisiting boundary layer flows of viscoelastic fluids. Journal of Non-Newtonian Fluid Mechanics, 312, 104976.

[3] Kousar, N. and Liao, S., (2011). Unsteady non-similarity boundary-layer flows caused by an impulsively stretching flat sheet. Nonlinear Analysis: Real World Applications, 12(1), 333-342.

[4] Merkin, J. H. and Kumaran, V., (2011). Free convection stagnation-point boundary-layer flow in a porous medium with a density maximum. International journal of thermal sciences, 50(11), 2176-2183.

[5] Bhattacharyya, K., Mukhopadhyay, S. and Layek, G. C., (2011). Steady boundary layer slip flow and heat transfer over a flat porous plate embedded in a porous media. Journal of Petroleum Science and Engineering, 78(2), 304-309.

[6] Khan, M. and Azam, M., (2016). Unsteady boundary layer flow of Carreau fluid over a permeable stretching surface. Results in Physics, 6, 1168-1174.

[7] Rauf, A., Siddiq, M. K., Abbasi, F. M., Meraj, M. A., Ashraf, M. and Shehzad, S. A., (2016). Influence of convective conditions on three dimensional mixed convective hydromagnetic boundary layer flow of Casson nanofluid. Journal of Magnetism and Magnetic Materials, 416, 200-207.

[8] Krishna, M. V. and Reddy, M. G., (2018). MHD free convective boundary layer flow through porous medium past a moving vertical plate with heat source and chemical reaction. Materials Today: Proceedings, 5(1), 91-98.
[9] Liu, L. and Liu, F., (2018). Boundary layer flow of fractional Maxwell fluid over a stretching sheet with variable thickness. Applied Mathematics Letters, 79, 92-99.

[10] Reddy, Y. D., Goud, B.S. and Kumar, M. A., (2021). Radiation and heat absorption effects on an unsteady MHD boundary layer flow along an accelerated infinite vertical plate with ramped plate temperature in the existence of slip condition. Partial Differential Equations in Applied Mathematics, 4, 100166.

[11] Ibrahim, W., & Makinde, O. D. (2013). The effect of double stratification on boundary layer flow and heat transfer of nano fluid over a vertical plate. Computers & Fluids, 86, 433-441.

[12] Mukhopadhyay, S. (2013). MHD boundary layer ow and heat transfer over an exponentially stretching sheet embedded in a thermally strati ed medium. Alexandria Engineering Journal, 52(3), 259-265

[13] Sekhar K. C. (2014). Boundary layer phenomena of MHD flow and heat and mass transfer over an exponentially stretching sheet embedded in thermally stratified medium. International Journal of Science, Engineering and Technology Research (IJSETR), 3(10), 2715-2721.

[14] Singh K., & Kumar M. (2015). The effect of chemical reaction and double stratification on MHD free convection in a Micro Polar fluid with heat generation and Ohmic heating. Journal of Mechanical and Industrial Engineering (JJMIE), 9(4), 279-288.

[15] Rehman, K. U., Khan, A. A., Malik, M. Y., & Pradhan, R. K. (2017). Combined effects of Joule heating and chemical reaction on non-Newtonian fluid in double strati ed medium: A numerical study. Results in physics, 7, 3487-3496.

[16] Kandasamy, R., Dharmalingam, R., & Prabhu, K. S. (2018). Thermal and solutal stratification on MHD nano fluid ow over a porous vertical plate. Alexandria engineering journal, 57(1), 121-130.

[17] Ahmad, S., Farooq, M., Javed, M., & Anjum, A. (2018). Double stratification effectsin chemically reactive squeezed Sutterby fluid ow with thermal radiation and mixed convection. Results in physics, 8, 1250-1259.

[18] Bilal, M., & Nazeer, M. (2021). Numerical analysis for the non-Newtonian flow over stratified stretching/shrinking inclined sheet with the aligned magnetic eld and nonlinear convection. Archive of Applied Mechanics, 91(3), 949-964.

[19] Reddappa, B. (2021). Analysis of the boundary layer flow of thermally conducting Jeffrey Fluid over a stratified exponentially stretching sheet. Turkish Journal of Computer and Mathematics Education (TURCOMAT), 12(13), 730-739.

[20] Khan, Q., Farooq, M., Ahmad, S., Alotaibi, H. and Muhammad, T., (2022). Analysis of squeezing flow of Powell–Eyring fluid with generalized transport phenomena and double stratification past inclined parallel sheets. Waves in Random and Complex Media, 32(6), 3095-3114.

[21] Borrelli, A., Giantesio, G. and Patria, M. C., (2015). MHD orthogonal stagnation-point flow of a micropolar fluid with the magnetic field parallel to the velocity at infinity. Applied Mathematics and Computation, 264, 44-60.

[22] Fauzi, N. F., Ahmad, S. and Pop, I., (2015). Stagnation point flow and heat transfer over a nonlinear shrinking sheet with slip effects. Alexandria Engineering Journal, 54(4), 929-934.

[23] Merkin, J. H. and Pop, I., (2018). Stagnation point flow past a stretching/shrinking sheet driven by Arrhenius kinetics. Applied Mathematics and Computation, 337, 583-590.

[24] Shafiq, A., Hammouch, Z. and Turab, A., (2018). Impact of radiation in a stagnation point flow of Walters' B fluid towards a Riga plate. Thermal Science and Engineering Progress, 6, 27-33.

[25] Khan, M., Sardar, H. and Gulzar, M. M., (2018). On radiative heat transfer in stagnation point flow of MHD Carreau fluid over a stretched surface. Results in physics, 8, 524-531.

[26] Abbas, N., Malik, M. Y., Alqarni, M. S. and Nadeem, S., (2020). Study of three-dimensional stagnation point flow of hybrid nanofluid over an isotropic slip surface. Physica A: Statistical Mechanics and its Applications, 554, 124020.

[27] Khan, M. I., Nigar, M., Hayat, T. and Alsaedi, A., (2020). On the numerical simulation of stagnation point flow of non-Newtonian fluid (Carreau fluid) with Cattaneo-Christov heat flux. Computer Methods and Programs in Biomedicine, 187, 105221.

[28] Hayat, T., Khan, S. A., Khan, M. I., Momani, S. and Alsaedi, A., (2020). Cattaneo-Christov (CC) heat flux model for nanomaterial stagnation point flow of Oldroyd-B fluid. Computer Methods and Programs in Biomedicine, 187, 105247.

[29] Wahid, N. S., Arifin, N. M., Pop, I., Bachok, N. and Hafidzuddin, M. E. H., (2022). MHD stagnation-point flow of nanofluid due to a shrinking sheet with melting, viscous dissipation and Joule heating effects. Alexandria Engineering Journal, 61(12), .12661-12672.

[30] Rehman, S., Anjum, A., Farooq, M. and Malik, M. Y., (2022). Melting heat phenomenon in thermally stratified fluid reservoirs (Powell-Eyring fluid) with joule heating. International Communications in Heat and Mass Transfer, 137, 106196.

[31] Ramzan, M., Farooq, M., Alsaedi, A. and Hayat, T., (2013). MHD three-dimensional flow of couple stress fluid with Newtonian heating. The European Physical Journal Plus, 128, 1-15.

[32] Waqas, M., Hayat, T., Farooq, M., Shehzad, S. A. and Alsaedi, A., (2016). Cattaneo-Christov heat flux model for flow of variable thermal conductivity generalized Burgers fluid. Journal of Molecular Liquids, 220, 642-648.

[33] Hayat, T., Qayyum, S., Farooq, M., Alsaedi, A. and Ayub, M., (2017). Mixed convection flow of Jeffrey fluid along an inclined stretching cylinder with double stratification effect. Thermal Science, 21(2), 849-862.

[34] Hayat, T., Ullah, I., Farooq, M. and Alsaedi, A., (2019). Analysis of non-linear radiative stagnation point flow of Carreau fluid with homogeneous-heterogeneous reactions. Microsystem Technologies, 25, 1243-1250.

[35] Farooq, M., Ahmad, S., Javed, M. and Anjum, A., (2018). Magnetohydrodynamic flow of squeezed Maxwell nano-fluid with double stratification and convective conditions. Advances in Mechanical Engineering, 10(9), 1687814018801140.

[36] Javed, M., Farooq, M., Ahmad, S. and Anjum, A., (2019). Melting Heat Transfer in Thermally Stratified Magnetohydrodynamic Flow of Eyring-Powell Fluid with Homogeneous-heterogeneous Reaction. Journal of Magnetics, 24(2), 202-211.

[37] Hazeri-Mahmel, N., Shekari, Y. and Tayebi, A., (2021). Three-dimensional analysis of forced convection of Newtonian and non-Newtonian nanofluids through a horizontal pipe using single-and two-phase models. International Communications in Heat and Mass Transfer, 121, 105119.

[38] Tizakast, Y., Kaddiri, M. and Lamsaadi, M., (2021). Double-diffusive mixed convection in rectangular cavities filled with non-Newtonian fluids. International Journal of Mechanical Sciences, 208, 106667.

[39] Saini, A. K., Chauhan, S. S. and Tiwari, A., (2021). Creeping flow of Jeffrey fluid through a swarm of porous cylindrical particles: Brinkman–Forchheimer model. International Journal of Multiphase Flow, 145, 103803.

[40] Malik, H. T., Farooq, M. and Ahmad, S., (2021). Significance of nonlinear stratification in convective Falkner-Skan flow of Jeffrey fluid near the stagnation point. International Communications in Heat and Mass Transfer, 120, 105032.

[41] Farooq, J., Chung, J. D., Mushtaq, M., Lu, D., Ramazan, M. and Farooq, U., (2018). Influence of slip velocity on the flow of viscous fluid through a porous medium in a permeable tube with a variable bulk flow rate. Results in Physics, 11, 861-868.

[42] Soomro, F. A., Usman, M., Haq, R. U. and Wang, W., (2018). Thermal and velocity slip effects on MHD mixed convection flow of Williamson nanofluid along a vertical surface: Modified Legendre wavelets approach. Physica E: Low-dimensional Systems and Nanostructures, 104, 130-137.

[43] Nojoomizadeh, M., Karimipour, A., Firouzi, M. and Afrand, M., (2018). Investigation of permeability and porosity effects on the slip velocity and convection heat transfer rate of Fe3O4/water nanofluid flow in a microchannel while its lower half filled by a porous medium. International Journal of Heat and Mass Transfer, 119, 891-906.

[44] Ahmad, S., Yousaf, M., Khan, A. and Zaman, G., (2018). Magnetohydrodynamic fluid flow and heat transfer over a shrinking sheet under the influence of thermal slip. Heliyon, 4(10), 00828.

[45] Khan, M. I., Kadry, S., Chu, Y. and Waqas, M., (2021). Modeling and numerical analysis of nanoliquid (titanium oxide, graphene oxide) flow viscous fluid with second order velocity slip and entropy generation. Chinese Journal of Chemical Engineering, 31, 17-25.

[46] Rahmati, A. R. and Derikvand, M., (2020). Numerical study of non-Newtonian nano-fluid in a micro-channel with adding slip velocity and porous blocks. International Communications in Heat and Mass Transfer, 118, 104843.

[47] Shah, S. and Hussain, S., (2021). Slip effect on mixed convective flow and heat transfer of magnetized UCM fluid through a porous medium in consequence of novel heat flux model. Results in Physics, 20, 103749.

[48] Yusuf, T. A., Kumar, R. N., Prasannakumara, B. C. and Adesanya, S. O., (2021). Irreversibility analysis in micropolar fluid film along an incline porous substrate with slip effects. International Communications in Heat and Mass Transfer, 126, 105357.

[49] Obalalu, A. M., Ajala, O. A., Abdulraheem, A. and Akindele, A. O., (2021). The influence of variable electrical conductivity on non-Darcian Casson nanofluid flow with first and second-order slip conditions. Partial Differential Equations in Applied Mathematics, 4, 100084.

[50] Adigun, J. A., Adeniyan, A. and Abiala, I. O., (2021). Stagnation point MHD slip-flow of viscoelastic nanomaterial over a stretched inclined cylindrical surface in a porous medium with dual stratification. International Communications in Heat and Mass Transfer, 126, 105479.

[51] Ullah, Z., Zaman, G. and Ishak, A., (2020). Magnetohydrodynamic tangent hyperbolic fluid flow past a stretching sheet. Chinese Journal of Physics, 66, 258-268.

[52] Jafar, A. B., Shafie, S. and Ullah, I., (2020). MHD radiative nanofluid flow induced by a nonlinear stretching sheet in a porous medium. Heliyon, 6(6), 04201.

[53] Fatunmbi, E. O. and Adeniyan, A., (2020). Nonlinear thermal radiation and entropy generation on steady flow of magneto-micropolar fluid passing a stretchable sheet with variable properties. Results in Engineering, 6, 100142.

[54] Prasannakumara, B. C., (2021). Numerical simulation of heat transport in Maxwell nanofluid flow over a stretching sheet considering magnetic dipole effect. Partial Differential Equations in Applied Mathematics, 4, 100064.

[55] Khan, U., Ishak, A. and Zaib, A., (2021). Hybrid nanofluid flow containing single-wall and multi-wall CNTs induced by a slender stretchable sheet. Chinese Journal of Physics, 74, 350-364.

[56] Khan, M. R., Elkotb, M. A., Matoog, R. T., Alshehri, N. A. and Abdelmohimen, M. A., (2021). Thermal features and heat transfer enhancement of a casson fluid across a porous stretching/shrinking sheet: analysis of dual solutions. Case Studies in Thermal Engineering, 28, 101594.

[57] Khan, U., Zaib, A., Bakar, S. A. and Ishak, A., (2021). Stagnation-point flow of a hybrid nanoliquid over a non-isothermal stretching/shrinking sheet with characteristics of inertial and microstructure. Case Studies in Thermal Engineering, 26, 101150.

[58] Zainal, N. A., Nazar, R., Naganthran, K. and Pop, I., (2021). Unsteady MHD stagnation point flow induced by exponentially permeable stretching/shrinking sheet of hybrid nanofluid. Engineering Science and Technology, an International Journal, 24(5), 1201-1210.

[59] Sarwar, N., Asjad, M. I., Hussain, S., Alam, M. N. and Inc, M., (2022). Inclined magnetic field and variable viscosity effects on bioconvection of Casson nanofluid slip flow over non linearly stretching sheet. Propulsion and Power Research.

[60] Mahabaleshwar, U.S., Vishalakshi, A. B. and Andersson, H. I., (2022). Hybrid nanofluid flow past a stretching/shrinking sheet with thermal radiation and mass transpiration. Chinese Journal of Physics, 75, 152-168.

[61] Liao, S., (2012). Homotopy analysis method in nonlinear differential equations (pp. 153-165). Beijing: Higher education press.

[62] Abbasbandy, S., Hashemi, M. S. and Hashim, I., (2013). On convergence of homotopy analysis method and its application to fractional integro-differential equations. Quaestiones Mathematicae, 36(1), 93-105.

[63] Turkyilmazoglu, M., (2012). Solution of the Thomas–Fermi equation with a convergent approach. Communications in Nonlinear Science and Numerical Simulation, 17(11), 4097-4103.

[64] Khan, M. and Khan, W. A., (2016). Three-dimensional flow and heat transfer to burgers fluid using Cattaneo-Christov heat flux model. Journal of Molecular Liquids, 221, 651-657.

[65] Hayat, T. and Sajid, M., (2007). On analytic solution for thin film flow of a fourth-grade fluid down a vertical cylinder. Physics Letters A, 361(4-5), 316-322.

[66] Hayat, T., Farooq, M. and Alsaedi, A., (2015). Thermally stratified stagnation point flow of Casson fluid with slip conditions. International Journal of Numerical Methods for Heat & Fluid Flow, 25(4), 724-748.

[67] Hassan, H. and Mehdi Rashidi, M., (2014). An analytic solution of micropolar flow in a porous channel with mass injection using homotopy analysis method. International Journal of Numerical Methods for Heat & Fluid Flow, 24(2), 419-437.

[68] Hayat, T., Ali, S., Awais, M. and Alhuthali, M.S., (2015). Newtonian heating in stagnation point flow of Burgers fluid. Applied Mathematics and Mechanics, 36, 61-68.

[69] Zhu, J., Yang, D., Zheng, L. and Zhang, X., (2016). Effects of second order velocity slip and nanoparticles migration on flow of Buongiorno nanofluid. Applied Mathematics Letters, 52, 183-191.

[70] Rehman, S. U., Mir, N. A., Farooq, M., Rafiq, N. and Ahmad, S., (2022). Analysis of thermally stratified radiative flow of Sutterby fluid with mixed convection. Proceedings of the Institution of Mechanical Engineers, Part C: Journal of Mechanical Engineering Science, 236(2), 934-942.

[71] Agbaje, T. M., Mondal, S., Makukula, Z. G., Motsa, S. S. and Sibanda, P., (2018). A new numerical approach to MHD stagnation point flow and heat transfer towards a stretching sheet. Ain Shams Engineering Journal, 9(2), 233-243.

[72] Fox, R. W., McDonald, A. T., & Pitchard, P. J. (2006). Introduction to fluid mechanics, 2004.

[73] Cengel, Y., & Cimbala, J. (2013). Ebook: Fluid mechanics fundamentals and applications (si units). McGraw Hill.

[74] Bansal, D. R. (2010). A Textbook of Fluid Mechanics and Hydraulic Machines, Laxmi Publications.

[75] Bansal, R. K. (2005). A textbook of fluid mechanics. Firewall Media.

[76] Reddy, J. N., & Gartling, D. K. (2010). The finite element method in heat transfer and fluid dynamics. CRC press.

[77] Ahmed, J., & Rahman, M. S. (Eds.). (2012). Handbook of food process design, 2 Volume Set. John Wiley & Sons.

[78] Cengel, Y., & Cimbala, J. (2006). Momentum analysis of flow system, fluid mechanics fundamentals and applications. Mcgraw Hill higher education 227-268.

[79] Molokov, S. S., Moreau, R., & Moffatt, H. K. (Eds.). (2007). Magnetohydrodynamics: Historical evolution and trends (Vol. 80). Springer Science & Business Media.

[80] White, F. M., & Corfield, I. (2006). Viscous Fluid Flow, vol. 3 McGraw-Hill. New York.

[81] Gad-el-Hak, M. (Ed.). (2013). Frontiers in experimental fluid mechanics (Vol. 46). Springer Science & Business Media.

[82] Papanastasiou, T., Georgiou, G., & Alexandrou, A. N. (1999). Viscous fluid flow. CRC press.

[83] Cleland, D. J. (2005). Moisture and humidity control in refrigerated facilities. Encyclopaedia of Agricultural, Food and Biological Engineering, 1-4.